University of Kentucky

UKnowledge

University of Kentucky Master's Theses

Graduate School

2010

DISTRACTION OSTEOGENESIS IN AN ORGAN CULTURE MODEL

Bradley R. Heil
University of Kentucky, brad.heil@uky.edu

Right click to open a feedback form in a new tab to let us know how this document benefits you.

Recommended Citation

Heil, Bradley R., "DISTRACTION OSTEOGENESIS IN AN ORGAN CULTURE MODEL" (2010). *University of Kentucky Master's Theses*. 47.
https://uknowledge.uky.edu/gradschool_theses/47

This Thesis is brought to you for free and open access by the Graduate School at UKnowledge. It has been accepted for inclusion in University of Kentucky Master's Theses by an authorized administrator of UKnowledge. For more information, please contact UKnowledge@lsv.uky.edu.

ABSTRACT OF THESIS

DISTRACTION OSTEOGENESIS IN AN ORGAN CULTURE MODEL

Distraction osteogenesis (DO) is a surgical procedure in which applied strain stimulates new bone growth; however, the underlying mechanisms by which bone cells respond to load are still uncertain. An organ culture model of DO was developed and validated by using linear distraction on the femoral shafts of 5 day old Wistar rats. Two loading regimes were utilized: distracting the bones for 2 hrs on day 1 (GRP I); distracting the bones for 2 hrs on days 1, 3, and 5 (GRP II). After 1 week in culture, the bones were compared to unloaded contralateral controls and assessed for changes. Structural, dimensional, massing, micro-CT, areal, and viability properties were obtained from testing. Relative to paired controls, distracted bones demonstrated an increase in failure load (9.15% GRP I, 18.85% GRP II), increase in stiffness (31.28% GRP I, 53.21% GRP II), increases in areal and polar moments of inertia, and viability (6.21% GRP I, 13.02% GRP II). Our results suggest that DO can be modeled successfully with an organ culture, and continued use of this system will help to gain insight into the mechanisms and pathways by which distraction osteogenesis occurs.

Bradley R. Heil
August 2010

DISTRACTION OSTEOGENESIS IN AN ORGAN CULTURE MODEL

By

Bradley R. Heil

Marnie M. Saunders, PhD
Director of Thesis

Abhijit Patwardhan, PhD
Director of Graduate Studies

August 2010

RULES FOR USE OF THESIS

Unpublished theses submitted for the Master's degree and deposited in the University of Kentucky Library are as a rule open for inspection, but are to be used only with due regard to the rights of the authors. Bibliographical references may be noted, but quotations or summaries of parts may be published only with the permission of the author, and with the usual scholarly acknowledgments.

Extensive copying or publication of the thesis in whole or in part also requires the consent of the Dean of the Graduate School of the University of Kentucky.

A library that borrows this thesis for use by its patrons is expected to secure the signature of each user.

<u>Name</u>   <u>Date</u>

_____

_____

_____

_____

_____

_____

_____

_____

_____

_____

_____

_____

Thesis

Bradley R. Heil

The Graduate School

University of Kentucky

2010

DISTRACTION OSTEOGENESIS IN AN ORGAN CULTURE MODEL

_____

THESIS

_____

A thesis submitted in partial fulfillment of the requirements
for the degree of Master of Science in Biomedical Engineering
in the Graduate school at the University of Kentucky

By

Bradley R. Heil

Lexington, Kentucky

Director: Dr. Marnie M. Saunders, Assistant Professor of Biomedical Engineering

Lexington, Kentucky

2010

ACKNOWLEDGEMENTS

I would first like to acknowledge my parents for everything they have done for me, not just while at the University of Kentucky, but throughout my life. They have been sources of guidance and inspiration.

I would also like to thank my advisor Dr. Marnie Saunders for her help and support during my time at UK.

A huge thanks goes out to Linda Simmerman with whom most of my days in the lab were spent. Not only did she help me with the day to day dealings of the lab, she was also vital with the viability study. She also provided me someone with whom I could talk UK sports, and for that, I am truly grateful.

Special thanks to Cynthia Long with her help in cryostat sectioning and Katelyn Gurley with the micoCT.

Table of Contents

iv

LIST OF TABLES

LIST OF FIGURES

1 Introduction

Distraction osteogenesis (DO) is a clinical procedure capable of generating viable osseous tissue by the gradual separation of osteotomized bone edges [1]. At the cellular level, it is a controlled mechanical procedure that initiates a regenerative process and uses mechanical strain to enhance the biological responses of the cells in and around the injured tissues to create new bone [2]. The clinical application of this process has gained wide acceptance for treating limb deformities, reconstruction of large bony defects, and fracture nonunions or malunions [3]. This clinical technique has been performed in orthopedic settings as mentioned, but it also has a valuable use as a technique for correcting craniofacial deformities.

Numerous experimental models have been developed to define the technical principles of distraction osteogenesis, however, the molecular mechanisms guiding successful generate bone formation remain unknown [4]. Additionally, the underlying cellular mechanisms of distraction osteogenesis are poorly understood [5] and very few of these experimental models have incorporated the use of an organ culture model. To gain a better understanding of the mechanisms underlying distraction osteogenesis, this study aims to create a model of distraction osteogenesis using neonatal rat femurs as an organ culture system. It has been shown that tension stresses promote bone formation in osteogenic tissue in vitro [6]. By combining distraction osteogenesis and an organ culture model, this study intends to see if tension stresses promote bone formation ex vivo. Further testing using this model will hope to reveal if linear distraction has other effects on bone or bone cells in an organ culture model. Continued use of this model

1

after this experiment may help to gain an understanding of the pathways and mechanisms by which bone cells respond to load.

2 Background

2.1 Organ Culture Model

An organ culture model is one where an entire organ is removed from the body and studied ex vivo. There are two other models that are often used for experimentation, the first of which is the in vivo model, or the animal model. The second is the in vitro, or cell model, a system in which the study takes place outside the body and usually involves cells cultured in petri dishes, flasks, or test tubes. All three models have their own advantages and disadvantages, and a culturing method should be chosen based on the needs and limitations of the desired experiment.

There are several reasons why an ex vivo organ culture model was chosen for this particular experiment over the other models. As Saunders explains, using an organ culture modeling approach, whole bone maintained in culture may be subjected to stimulation and the effect of the stimulation assessed in a physiologic milieu maintaining appropriate cell types and numbers within their 3D, communication-intact environment [7]. By removing the bone from the rest of the body, systemic effects from other areas of the body were eliminated. The removal of systemic effects was not possible for an in vivo model. Organ culture models also provide a means to create a highly biomimetic environment. Through the control of temperature and CO_2 (%), both of which can be fine-tuned for particular needs, the organ culture tries to mimic the natural environment inside the body.

Although not as common as in vivo or in vitro studies, a wide range of organ culture studies have been done for different organs within different animals. Some of the animals that have been studied using organ culture systems are rats [7, 8, 9, 10, 11, 12,

13, 14, 15], mice [16, 17, 18], humans [10, 19, 20, 21, 22], cows [22], rabbits [23], and pigs [24]. Some of the organs and tissues that have been studied using organ culture systems are arteries [8, 10, 11, 12, 19, 20, 21, 23, 24, 25], cartilage [16, 18, 26, 27], pancreatic ducts [22], diaphragms [15, 17], colons [13], skeletal muscle [14], and the liver [9]. All of these sources with different organs from a variety of animals exhibit the diversity of the organ culture model. The organ culture in use for this study has also been previously validated [7].

Studies involving distraction osteogenesis using an organ culture model have previously been examined. In 2000, Matsuno et. al, analyzed the cellular response to the mechanical stress of distraction osteogenesis by histological evaluations [28]. By fixing the sample with a dental reamer and using a micrometer to distract the bone samples, they were the first to publish results of a tissue cultured distraction osteogenesis experiment. The results of their experiment still left much to be considered, mainly because they looked strictly at the histology within the regenerated bone with no regard for the rest of the bone. Our study aims to look at the bone as a complete tissue and to analyze the properties of the entire bone. Matsuno's study also looked at an older bone (5 weeks) that required an in vivo fracture whereas this study will eliminate the fracture by using a much younger animal.

2.2 Bone Physiology

Bone is a natural composite material consisting of approximately 60% mineral, 10% water and 30% collagenous matrix with the quality and interaction of these constituents playing a major role in determining the mechanical behavior of bone [29]. There are three different types of bone cells: osteoblasts, osteoclasts, and osteocytes [30].

4

Osteoblasts are the bone cells that lay down new bone, while the osteoclasts are bone cells that remove bone. The osteoblasts and osteoclasts work together to continually remodel healthy bone. Osteocytes are mature osteoblasts that have been enclosed in fully formed bone and will play a major role in determining the viability of the bone, a topic discussed in Chapter 3.

Two types of bone of present in the body: cortical and cancellous [30]. Cortical bone, also referred to as compact bone, can be found along the outer portion of most of the bones in the body. It is typically harder and stronger than cancellous bone, and thus provides much of the support and protection for the body. Cancellous bone, also called spongy or trabecular bone, is much less dense than cortical bone and is found on the interior portions of bones, where it functions mostly in metabolic activities [31]. Both types of bones have the ability to respond to loading, but cancellous bone responds better to stimuli than cortical bone [32]. This is due to the increased porosity cancellous bone has over cortical bone leading to an increased surface area. Not only does bone respond to loading, it also has a substantial capacity for repair and regeneration in response to injury or surgical treatment [2]. Since one of the aims of this study is to model distraction osteogenesis, only the cortical bone on the bone's shaft will be analyzed, as it is the bone area that is distracted during the clinical procedure.

As previously mentioned, cortical and cancellous bone have the ability to respond to loading. One of the principles related to bone's responsive ability is referred to as Wolff's Law. It states that bone is deposited and resorbed to achieve an optimum balance between strength and weight and that this occurs through self-regulating mechanisms that respond to mechanical forces acting upon bone tissues [33,34,35]. Wolff, a German

surgeon and anatomist during the 19th century, suggested that if loading on a bone increased, the bone would respond and remodel itself to withstand the load. An example of Wolff's Law in action can be seen below in Figure 2.2.1. The figure shows an x-ray image of the forearms of a right handed professional tennis player. The right forearm, the dominant forearm, shows thicker and denser bone due to the bone responding to the increased loading. The converse of this process can be seen in astronauts who spend long periods of time in space with no loading due to gravity. Upon returning to Earth, the astronauts' muscles and bones are atrophied due to the reduced load on their bones [36]. In this experiment, bone's response to the mechanical stimulation it experiences during distraction osteogenesis will be examined.

Figure 2.2.1 Forearms of a right handed professional tennis player with hypertrophy of the right arm [37]

2.3 Distraction Osteogenesis

Distraction osteogenesis is the gradual lengthening of bone by applying controlled mechanical force in order to separate osteotomised bone segments [38]. Distraction

osteogenesis induces new bone formation along the vector of pull without requiring the use of bone graft [39]. The first mention of a distraction osteogenic process came in 1905 by the Italian surgeon Alessandro Codivilla [40], who, during his surgical procedures, used tensile force to distract the bone to perform a limb-lengthening procedure to correct deformities. Although rudimentary, it was the first step towards understanding distraction osteogenesis.

Distraction osteogenesis takes place over the course of three phases. The first phase is the latency period immediately following the fracture of the bone (either osteotomy or corticotomy) which allows for healing. As the bone is healing, the two pieces are slowly pulled apart in a controlled manner, a process known as the distraction phase. If the bone is pulled apart too quickly, it may not be able to form in between the two pieces and a fibrous cartilage union will result. If the bone is distracted too slowly, it will result in an early consolidation with bone forming across the distraction gap before the desired length is reached [41]. Not only is the speed of the distraction important to how the bone grows and forms between the two bone segments, but the rigidity of the fixation hardware also affects the bone growth [42]. As the new bone is being formed in the distraction gap, it forms centripetally from the edges of the bone towards the middle of the distraction gap [43]. The consolidation phase is the final phase of distraction osteogenesis, occurring when the bone that has formed centripetally between the two bone segments becomes mineralized.

In vitro studies of distraction osteogenesis have shown effects on a cellular level. Mouse calvarial MC3T3 cells that were suspended in a polymerized three-dimensional collagen gel and stressed for 14 days at a distraction rate of 0.5 mm/day showed that

morphologic changes can occur over time such that linear distraction forces cause cells to elongate and align in a parallel direction to the force [5]. This process involved distraction forces, but the idea of cells aligning along the direction of loading is not a new concept. In 1942, Glucksmann published his results showing the histological structure of developing bone in vitro is orientated along the lines of tension in osteogenic tissue [6]. Another in vitro study showed that osteoblasts that had undergone a 3% uniaxial strain for 8 hours assumed a fusiform, spindle-shaped morphology as compared to the unstrained osteoblasts which appeared to have a stellate appearance and haphazard arrangement [4]. Similar results from in vivo studies specific to distraction osteogenesis showed that bone trabeculae and fibrous tissue were aligned in the direction of the vector of distraction [38] as well as that cells residing within the distraction gap align parallel to the vector of distraction [44]. Figure 2.3 shows results from Bhatt's in vitro study.
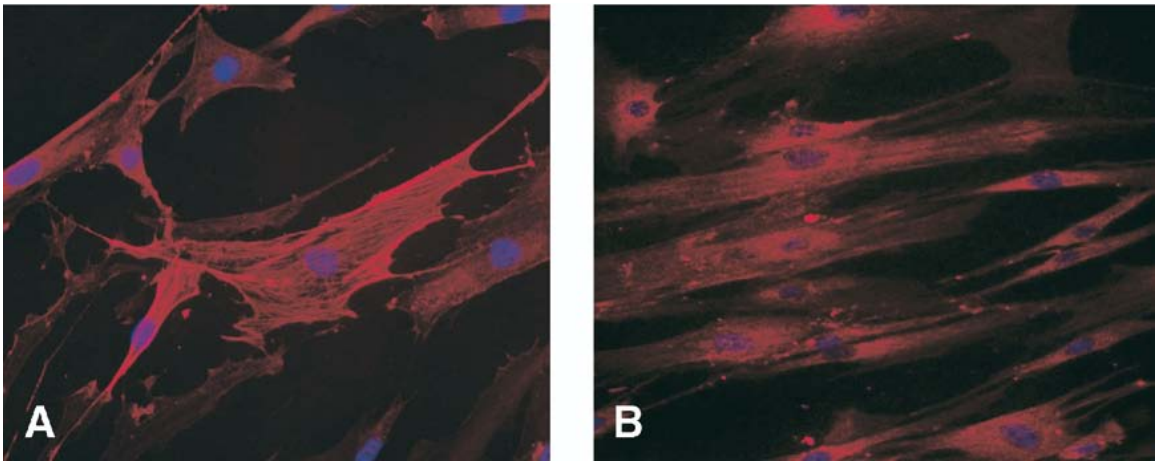
Figure 2.3 Unstrained (A) and strained (B) osteoblasts demonstrate differences in cellular alignment [4].

Distraction provides a pulsed form stimulation by tension stresses across the osteotomy site, and it also initiates osteogenesis [45]. The osteomoty site is also

8

important because the mechanical environment around the osteotomy site is one of the main factors that affects both quantity and quality of the regenerated bone [3]. However, in certain cases, mostly those involving neonates, an osteotomy is not always needed for distraction osteogenesis to occur. In these cases, the bone is soft enough, but more importantly it is osteogenic enough, to distract without the osteotomy site. Staffenberg et al, first showed that an osteotomy was not needed in midface distraction in a canine model [46]. A human case where osteotomies are not performed is an innovative surgical technique for midface distraction that is safe, efficient, minimally invasive, and seems best suited to patients in early infancy highlighted in a clinical study by Graewe [47]. In this study, an osteotomy will not be needed for the distraction method, as the two ends of the bone shaft will be pulled in a linear fashion, creating the osteogenic effect necessary for bone growth to occur.

2.3.1 Strain

Strain, the fundamental mechanism of distraction osteogenesis, is a mechanical property defined as the deformation of a material relative to its own dimensions [48]. Engineering strain is measured by taking the change in length of an object (displacement) and dividing it by the original length of that object. The units of length cancel out leaving strain as a unit-less property, but it is most commonly measured in micro-strain ($10E^{-6}$). Much of bone's behavior can be determined and is dictated by the level of strain [49]. Osteocytes are rapidly responsive to mechanical events in their surrounding tissue in a peak strain magnitude-dependent manner [50] and therefore it is believed that the osteocytes sense and respond to strain. It is also believed that osteocytes that are mechanically stimulated through shear stress will regulate osteoblastic activity via gap

9

junctions [51], another example of the osteocytes' sense of loading. The development of this organ culture distraction system may lead to further studies involving the cellular response and interactions between osteocytes and osteoblasts.

The age of the bone being studied can vary the effects that strain has on bone. In a study done on elderly human tibiae, it was seen that few of the bones could survive more than a 1% change [52]. The strain level sought in this study is a 2% strain on the bone shaft, and although the results from Nyman's study seem to say that 2% strain would be too high, this study is dealing with a different bone from a different animal at a different age. In fact, the 2% strain on the bone is not too high since the bones being studied were able to withstand a 66% elongation (Section 3.2)

Another factor that can alter the affect that strain has on an object, particularly bone, is loading direction. It is known that changes in loading direction can change both stiffness and strength [53]. Even slight variations in the angle of loading can cause significantly different results, an effect very relative to how cells, trabeculae, and fibrous tissue will align in the direction of distraction as mentioned in section 2.3. The model used for this experiment represents the simplest form of distraction osteogenesis by using linear strain. This assures the loading direction is always along the long axis of the bone.

2.3.2 Clinical Relevance

While performing distraction osteogenesis procedures, surgeons must take into account several factors to help insure a safe and successful surgery [54]. The first is the blood supply to the bone and surrounding tissues as blood loss to these areas may result in necrosis of the bone or tissue. Other factors to be considered are the surrounding muscles and nerves and the possible involvement of hardware that could damage the

10

surrounding tissues or result in nerve paralysis. Care must be taken throughout the procedure to eliminate the possible damages.

Skin is another factor that influences distraction osteogenesis procedures. With external fixators, there is a greater risk for scarring once the fixation hardware is removed [55]. Hardware going through the skin also creates areas that are more susceptible to infection after the surgery. All of these factors and more are figured into the equation when surgeons determine both the style of procedure and type of hardware.

One of the more typical distraction osteogenesis procedures seen in the 1980's and 1990's was the Ilizarov method. Gavril Ilizarov was a Soviet physician who popularized distraction in the long bones of the legs. Through his research and clinical procedures, he created the Law of Tension-Stresses, which states that gradual traction on living tissues creates stresses that can stimulate and maintain the regeneration and active growth of certain tissue structures [56]. His procedure and techniques using an external ring fixator came to be known as the Ilizarov method.

One area that is often disputed among surgeons is how often to distract the bone per day. Different daily rates of distraction and frequencies of distraction may have an effect on both bone and soft tissues under the influence of tension-stress [41]. In many cases, the overall distraction takes place over several distractions per day, but it is not uncommon to see the use of anywhere from 1-4 distractions per day to achieve an overall distraction length. The distraction length that is most commonly seen in clinical settings is 1mm/day [3, 57, 58, 59], simply because distraction rates higher than 1 mm/day may have adverse effects [54]. Another possible distraction method is continuous distraction, a method in which the distraction is non-stop over a 24 hour period and is completely

automated [38]. Using continuous distraction osteogenesis in rabbits has shown

significantly more regenerated bone volume in the central part of the regenerated area

than the use of discontinuous distraction osteogenesis, while also producing higher

osteoblastic activity and more blood vessels [38]. Continuous distraction has other

advantages over discontinuous distraction. Since the distraction is automated, the

patients don't have to go to a clinic to have a doctor perform the distraction, and if the

patient performs the distraction themselves, human error can be avoided.

Although originally developed by orthopedic surgeons, distraction osteogenesis

has also been used on craniofacial bones (mandible, maxilla, etc) to treat congenital as

well as acquired craniofacial bone defects [38]. Synder et al were the first to use

mandibular distracation osteogenesis when they performed the procedure on a canine

mandible [60]. This procedure was first seen clinically on humans in 1989 when it was

performed on four young patients with an average age of 78 months [61]. Since then,

distraction osteogenesis has become an accepted method in cranio-maxillofacial surgery

to treat severe deformity that could not be adequately corrected with other surgical

methods [62]. Distraction osteogenesis also allows for greater advances of distances

[47]. In cases of micrognathia, mandibular distraction osteogenesis was used to

effectively alleviate severe upper airway obstruction and in most cases, a tracheotomy

(the traditional and safest treatment option) was avoided [55]. Upper airway obstructions

were also alleviated by the previously mentioned technique of midface distraction [47].

As with orthopedic distraction osteogenesis, external or internal distractors can be used

for craniofacial distraction osteogenesis. Although internal distractors are technically

more challenging to apply due to the smaller working space, this method is preferred,

when feasible, because there is less chance of device dislodgment during consolidation

and there is no visible external hardware, which results in less visible facial scarring [55].

3 Materials and Methods

3.1 Organ Culture

3.1.1 Bone Harvesting

For this experiment, the bones of five day old Wistar rats were studied. These bones were chosen because they were not fully calcified, they were osteogenic, and distraction procedures have been done on infant bones without the need of an osteotomy [47]. After five days of birth, the pups were humanely euthanized using CO_2 in accordance with an approved protocol from the Institutional Animal Care and Use Committee at the University of Kentucky. Left and right femurs were extracted from the rats in a cell culture hood to maintain a sterile environment. One of the femurs was designated to be distracted (treated group) while the other was assigned to be the contralateral control (control group). Upon removal from the body, the soft tissue surrounding the femur was removed, and the bones were placed onto a stainless steel mesh bridge sitting in a well of a twelve well polystyrene tissue culturing plate (Becton Dickinson, Franklin Lakes, NJ) [7, 63]. Mesh bridges were used to keep the bones at the liquid air interface. The well was filled with medium to a level so that the tops of the condyles and femoral head were the only bone parts on top of the medium. Leaving the condyles above the medium allowed for gas exchange to occur at the bone-air interface. After all pairs of femurs had been removed and positioned in the wells, the plates were placed in an incubator at 37°C and 5% CO_2 for 24 hours to allow for equilibration since unintentional inflammatory responses may occur upon harvesting [64].
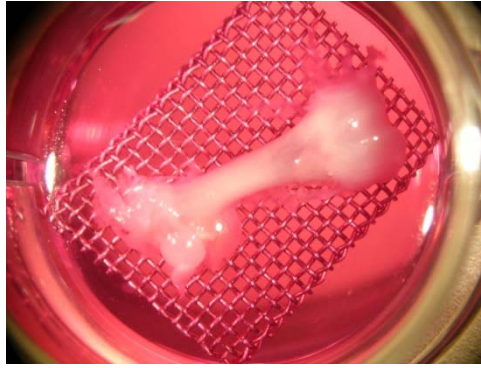
Figure 3.1.1: Image of femur laying on mesh bridge in the organ culture

3.1.2 Medium Feeding

To help maintain the viability of the bones and to avoid contamination, fresh medium feedings occurred every day. The medium that was used consisted of BGJb supplemented with 15% Fetal Bovine Serum (FBS) and 2% penicillin-streptomycin solution (pen-strep or P-S). The BGJb (Invitrogen, Carlsbad, CA) is a specific medium specially made to aid the development of bone organ cultures, while the FBS (Hyclone, Logan, UT) is the most widely used growth supplement for cell culture media because of its high content of embryonic growth promoting factors [65]. The Pen-Strep (Hyclone, Logan, UT) was used to help eliminate bacteria and reduce the possibility of contamination, which was a major concern during the project. Once the old medium had been removed, warmed medium (37°C) was pipetted into the wells to cover the entire bone except for the tops of the condyles and cartilage on the femoral head.

3.2 Bone Distraction

Linear tension was used to mimic the distraction osteogenesis process to create a 2% elongation of the bone shaft. The device used for this was a modified small-scale device fabricated in-house, whose original purpose was to calibrate liquid metal strain

gages. The device (see Figure 3.2a) had a rotating shaft that was able to be dialed in to

create a displacement with an accuracy of .0254 mm. The two ends of the suture of the

suture-wrapped femurs were clamped down on the rectangular blocks. The block on the

left was stationary whereas the block on the right was able to slide to the left or right.

The rod running through the block on the right was connected to the measuring dial. The

displacement distance would be dialed in, and the screw on the left would be manually

turned. Turning the screw on the left pushed the rod into the right block moving the

block to the right and providing the distraction to the bones.
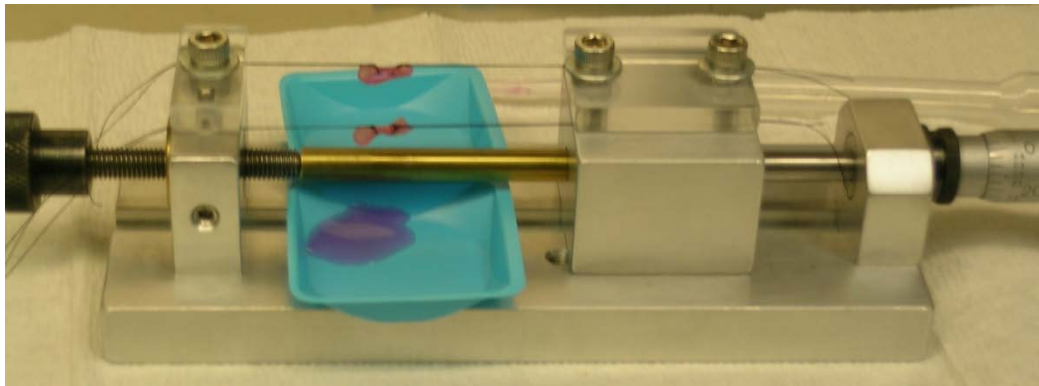
Figure 3.2a: Image of setup of the distraction device

To determine the distance of distraction necessary to achieve a 2% strain on the

bone shaft, two techniques were used. First, five day old Wistar rat shaft lengths from

previously tested bones were averaged (4.14 mm). To achieve a 2% strain based on the

average shaft length of the previously tested bones, the displacement distance would have

to be .0762 mm. To verify that a displacement distance of .0762 gave a 2% elongation on

the bone shaft, an optical technique was used. Pictures were taken before and after

distraction using several distraction distances, and after using image analysis software, it

was determined that a displacement distance of .0508 mm gave the most consistent 2% strain on the bone shaft.

The suture that was used to wrap the bones for this project was 5.0 .1mm thick non-absorbable, black braided silk suture that is typically used in orthopedic settings (Surgical Specialties Corporation, Reading, PA). Suture was used over a wire-wrapping procedure because of the possible deformation in the wire. The suture was cut to length (20.32 cm) and sterilized by autoclave, and a contamination study with the suture was conducted prior to testing. The suture was wrapped around the bone and kept in culture for one week. After one week in culture, no contamination was present, so the project continued. It must also be noted that no contamination was seen throughout the duration of this project.

Suture failure tests in tension were also conducted to determine the linear portion of the loading curve of the suture (see Figure 3.2b). The suture was pulled in tension until failure at three different speeds, and load displacement curves were created from the recorded data. The .0508 mm distraction distance was well within the linear region of the suture for all three speeds meaning that the suture would not break during the distraction process. To verify this, a tension test to failure was conducted with the bone. The bone was distracted and broke in the shaft after 2.794 mm (equivalent of a 67% elongation of the bone shaft) without the suture breaking. This showed that the suture would withstand the 2% elongation of the normal distraction loading.
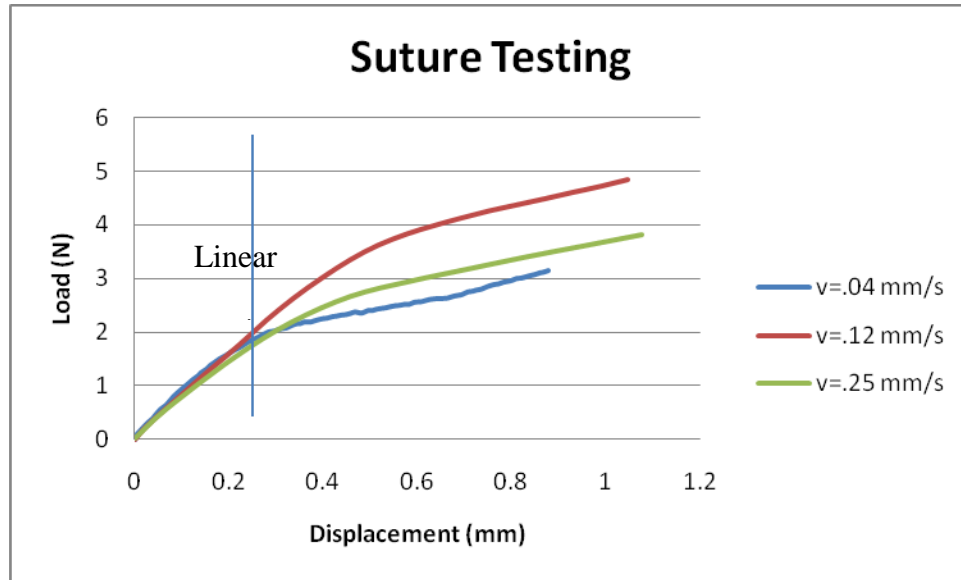
Figure 3.2b: Results of suture tension tests (3 speeds) showing the linear portion of the suture on a load displacement graph.

Two different loading regimes of the bones were analyzed. In the first group, GRP I, the treated bones were distracted a distance of .0.0508 mm and held for two hours on day 1. In the second group, GRP II, the treated bones were distracted a distance of .0508 mm and held for two hours on days 1, 3, and 5. This increase in the number of days the bones were distracted was done to increase the likelihood of eliciting a response. All of the distracted bones were paired with a contralateral control. To distract the bones, the sterile suture was lassoed around both ends of the femur bone shaft (See Figure 3.2) and the two ends of the suture were then pulled taut and clamped down in the distraction device. The bone was then distracted .0508 mm in one quick turn of the dial. The bone was held in place for two hours and medium droplets were added every 5 minutes to maintain adequate hydration of the bones. After completion of the two hours of distraction, the bones were returned to the organ culture, fresh medium was added, and

the bones were returned to the incubator. To ensure uniformity throughout the project, the distraction device was always reset before the next distraction occurred.
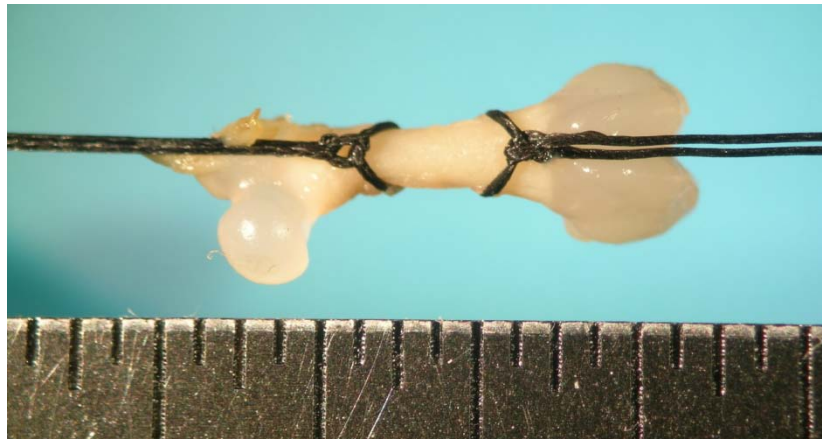
Figure 3.2c: Image of lassoing technique for distracting the bone shaft

An optical technique was used to verify that the bone shaft was maintained at the 2% elongation for the entire two hours. Pictures were taken at various time points throughout the two hours, and measurements were taken on the bone shaft to see if relaxation occurred. After reviewing the time lapse photos, it was determined that stress relaxation was occuring. After the two hours, the elongation that was originally 2% had decreased to 1.7%. Figure 3.2d below shows several of the time lapse photos.

19
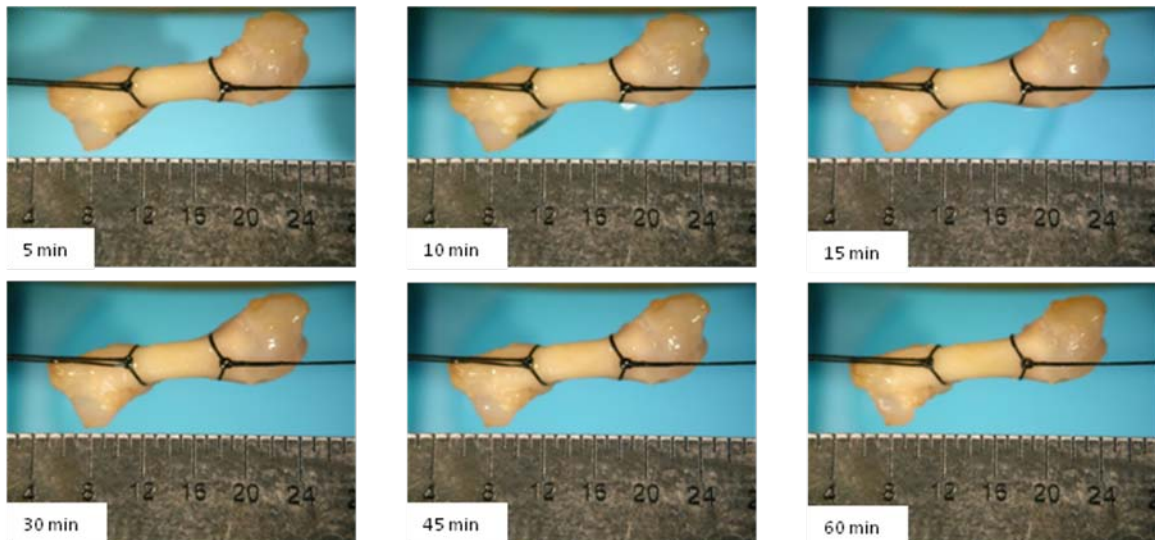
Figure 3.2d: Images from time lapse study showing stress relaxation of the original

2% elongation on the bone shaft over the two hour duration.

3.3 Bone Characterization

After one week in culture, the bones were tested in a variety of ways to give a general characterization of the bone (osteocyte viability, dimensions, masses, areal properties, and structural properties). To allow for a more random study, not all of the bones from one litter were tested the same way. This was done to try to eliminate effects of the size of the rat pups in the litter since not all litters would have the exact same sized rats. Regardless of the testing, the control and treated bone pair underwent the same characterization testing.

3.3.1 Lactate Dehydrogenase

Lactate dehydrogenase (LDH) is a catalytic enzyme that aides in the conversion of lactate to pyruvate during normal energy production in the cells [66, 67]. The absence of LDH in a cell means the cell is not metabolizing. By staining cells for LDH, it can be determined which cells are metabolizing and which are not, giving a good representation of the viability of the tissue. A protocol for assessing osteocyte viability using lactate dehydrogenase staining was developed using the previous work of Mann [66, 67]. The osteocytes were the obvious cell choice to measure viability because of the fact that they are housed in lacunae within the bone matrix and are easily imaged.

A stock base solution was made of 85 ml of Hanks Balanced Salt Solution (HBSS, Invitrogen, Carlsbad, CA), 5 gm of Polypep (Sigma P5155, St. Louis, MO), and 10 ml of a stock Gly-Gly (Sigma G3915, St. Louis, MO). The stock Gly-Gly was 264.24 mg gly-gly per 100 ml HBSS. 10 ml of the stock base solution was added to 17.5 mg of

Nictinamide AdenineDinucleotide (Fluka 43410, St. Louis, MO) and 100 μl of a stock

lactic acid (Sigma L1750, St. Louis, MO). The stock of the lactic acid was a 6M stock

created by mixing 5.4 g of lactic acid and 10 ml of deionized water. Once the reaction

chemicals reached a pH of 8.0, 3 tablets of Nitroblue Tetrazolium (Sigma N5514, St.

Louis, MO) were added. Once the Nitroblue Tetrazolium tablets were dissolved, the

bones were washed in warmed HBSS. Following the HBSS washings, the reaction

chemicals were added to the bones, which were then placed back into the incubator for 4

hours.

After 4 hours of incubation, the reaction chemicals were removed and the bones

were rinsed with deionized water. Four percent paraformaldehyde was added for 15

minutes while the bones were placed on a plate rocker. The bones were then placed in a

4°C refrigerator for 24 hours. After refrigeration, the bones were washed with deionized

water, and formic acid and EDTA decalcifier, Formical-2000 (Decal Chemical, Tallman,

NY), were added to the bones. The bones were left at room temperature for 24 hours,

and the decalcifying process was repeated until the bones became completely decalcified.

Complete decalcification was defined as the time point where no more calcium sediment

remained in solution (average of 5 days).

Once completely decalcified, the Formical-2000 was removed, the bones were

washed with dionized water, and they were stored at 4°C for a minimum of 24 hours in a

15% sucrose and dionized water solution. After refrigeration, the bones were cut into 8

micron thick longitudinal cross sections using a Shandon Cryotome FSE

(ThermoElectron Corporation) and mounted on glass slides. Once mounted, the slides

were heat treated for 1 hour at 45°C on a slide warmer.

Figure 3.3.1a: Image of LDH samples on glass slide prior to Methyl Green staining

Methyl green is a nuclear counter stain that turns the nuclei of cells light green

and in conjunction with the LDH, it provides a clearer representation of the cells'

location (vectorlabs.com). Two methyl green protocols were tried and reworked until the

best images could be obtained. The protocol selected was based off of Vector's

recommendation for their methyl green protocol on an individual slide [68]. A Liquid

Blocker Super PAP Pen (Daido Sangyo Co., Tokyo, Japan) was used to encircle the bone

slice that was to be studied and the glass slide was then heated to 60°C in the incubator

on a metal plate. Once the slide was heated, room temperature methyl green (Vector,

Burlingame, CA) was dropped on the slide inside the PAP circle to fully cover the bone.

After 5 minutes, the slide was placed in eosin for 30 seconds and then went through a

dehydration process accomplished by placing it in 95% EtOH for 5 minutes followed by

ten minutes in 100% EtOH (twice) and ten minutes in xylyne (three times). Once the

dehydration process was finished, a mounting media, Cytoseal 60 (Richard-Allan

Scientific, Kalamazoo, MI), was dropped on the sample, a cover slip was placed over the

slide, and the sample was ready to be counted.

Longitudinal cross-sections (6 per bone) were analyzed under a Nikon Eclipse

E600 light microscope (Nikon Instruments Inc., Melville, NY) for both control and

treated bones; pictures of the cross-sections were taken using a Nikon DN100 camera

(Nikon Instruments Inc., Melville, NY). Because of the variability in the location of the

osteocytes, the cortical bone on both the lateral and medial sides from distal to proximal

epiphysis was looked at under 60x magnification to obtain the most accurate counts (see

Figure 3.3.1b). Three parameters were determined by manual counts for each field of

view: the number of osteocytes in lacunae that showed traces of LDH (LDH +), the

number of osteocytes in lacunae that did not show any traces of LDH (LDH-), and the

number of empty lacunae where no osteocytes were present.
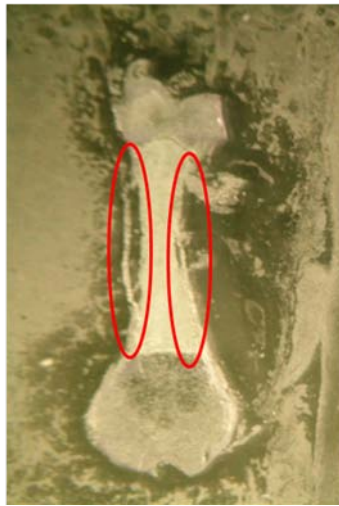
Figure 3.3.1b: Image taken of bone cross section marking the areas of the bone that were analyzed for osteocyte viability.
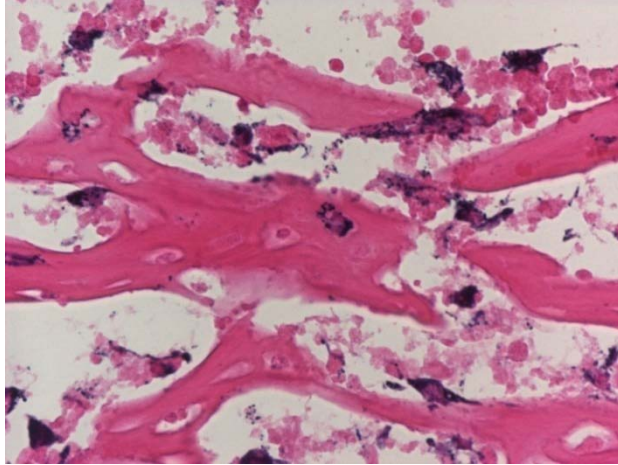
Figure 3.3.1c: Image taken of LDH samples with Nikon DN100 camera at 60X

magnification. The dark purple stain is LDH.

3.3.2 Dimensions

After one week in culture, pictures were taken of the distracted and control bones

to analyze dimensional changes in growth. Pictures were taken using a Nikon Coolpix

5400 digital camera along with a Nikon SMZ645 Dissecting microscope (Nikon

Instruments Inc., Melville, NY). A ruler was placed in the field of view to provide a

reference distance. Image J Software (NIH) was used to assess the dimensions. Three

measurements were taken of each bone: shaft diameter (SD), the shaft length (SL), and

the total length (TL). Shaft diameter was defined as the smallest distance between the

medial and lateral sides of the bone shaft. Shaft length was defined as the distance

between proximal and distal growth plates. Total length was defined as the distance from

the most proximal point on the femoral head to the most distal point on the condyles.

Figure 3.3.2 shows a picture of a femur with the dimensions labeled for better

understanding.
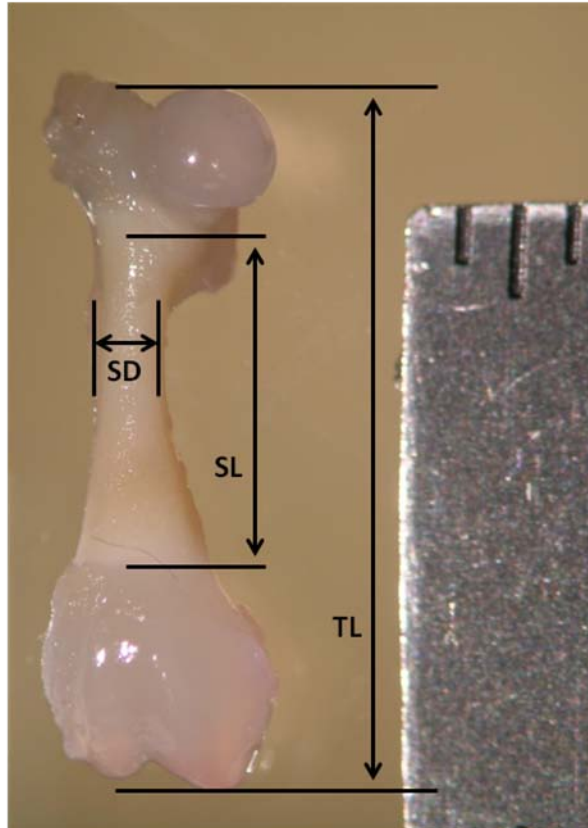
Figure 3.3.2: Image of femur with dimensional properties labeled. Shaft diameter (SD), shaft length (SL), and total length (TL) are labeled.

3.3.3 Mass

After one week in culture, the mass (g) of every bone was taken using a Sartorius CP64 scale (Sartorius, Germany). This mass was called the wet mass, which included water inside the bone and cartilage. The bones that were used to further analyze mass properties were then defatted in acetone for 72 hours, air dried for 24 hours, and heated in a furnace (FB1300 Barnstead International, Dubuque, IO) for 5 hours at 60°C to remove all of the water from the bones [69]. After the bones were cooled, they were massed to determine the dry mass. Following dry massing, the bones were placed in the furnace and heated to 600°C for 6 hours. After cooling, the bones were massed to obtain the ash

mash. At this point, the only remaining portions of the bone were composed of mineral.

Ash content was then found by dividing the ash mass by the dry mass and multiplying by

100 [69]. The ash content gave a representation of the percentage of bone that was

mineral.

Figure 3.3.3: Image of bone at time of wet massing (left). Image of bone at time of ash massing (right).

3.3.4 Areal Properties

To analyze cross-sectional properties, transverse slices of the bone shaft were

needed. To obtain these slices, the femurs were embedded in a self-curing acrylic

(Coralite Duz-all, Bosworth Company, Skokie, IL). Once the acrylic was fully hardened

and cooled (the reaction of the powder and liquid to form the acrylic is exothermic),

transverse slices of the femur shaft were obtained using an Isomet Low Speed saw

(Buehler, Lake Bluff, IL). Cross-sectional slices were cut to a thickness .89 mm. This

thickness was used because it allowed for consistent cutting and quality images.

Three measurements from a transverse slice from the middle part of the bone shaft were

taken to determine the outer diameter along the long axis, the outer diameter along the

short axis, the inner diameter along the long axis, and the inner diameter along the short axis. These dimensions were then used to calculate the cortical area (mm^2), medullary area (mm^2), area moment of inertia in the direction of the long axis (mm^4), area moment of inertia in the direction of the short axis (mm^4), and the polar moment of inertia (mm^4). The bone was simplified to the shape of an ellipse for the calculations of all these properties.
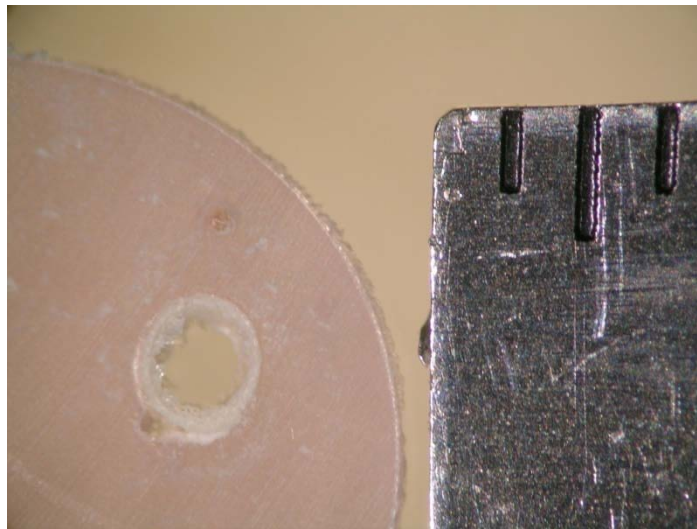
Figure 3.3.4a Image of transverse cross-section of bone embedded in bone cement

To determine the area of an ellipse, the following equation was used [70]

$$A = \pi ab$$

Where A is the area

a is the radius along the long axis

b is the radius along the short axis

The area of the hollow medullary cavity was calculated and called the medullary area. The total area of ellipse formed by the perimeter of the bone was also calculated. The

cortical area was then calculated by taking the total area and subtracting the medullary area.

To determine the area moments of inertia, the following equations were used [71]

$$I_x = \frac{\pi a b^3}{4}$$

$$I_y = \frac{\pi a^3 b}{4}$$

Where I_x is the area moment along the short axis

I_y is the area moment along the long axis

a is the radius along the long axis

b is the radius along the short axis

To determine the polar moment of inertia, the following equation was used [71]

$$J = \frac{\pi a b (a^2 + b^2)}{4}$$

Where J is the polar moment

a is the radius along the long axis

b is the radius along the short axis

The polar moment of inertia (pMOI) was also be found by adding I_x and I_y. Since the bone was assumed to be a hollow cylindrical ellipse, these equations had to be used twice to determine the actual moments for the bone shaft. The moments based on the dimensions for the medullary canal were subtracted from the moments based on the dimensions for the perimeter of the bone to give the actual areal and polar moments of inertia of the bone. These properties were all found on the assumption of the bone shaft

28

as a hollow cylindrical ellipse, but the shaft could also be approximated as a hollow cylinder. With this in mind, the area moments of inertia were also calculated using cylindrical formulas.

The areal properties were also found by using a MicroCT-40 computed tomography scanner (Scanco Medical, Basserdorf, Switzerland). Micro CT samples were prepared by fixation in formalin for 48 hours followed by storing at 4°C in 70% Ethanol [72]. Bones were scanned using source settings of 55 kV, 145 µA and high resolution [73]. Each scan produced 50, 2D axial slices in the midshaft of the bone. The areal, inertial, volumetric, and density properties were then determined over the 50 scan region as well as over the entire femoral shaft.
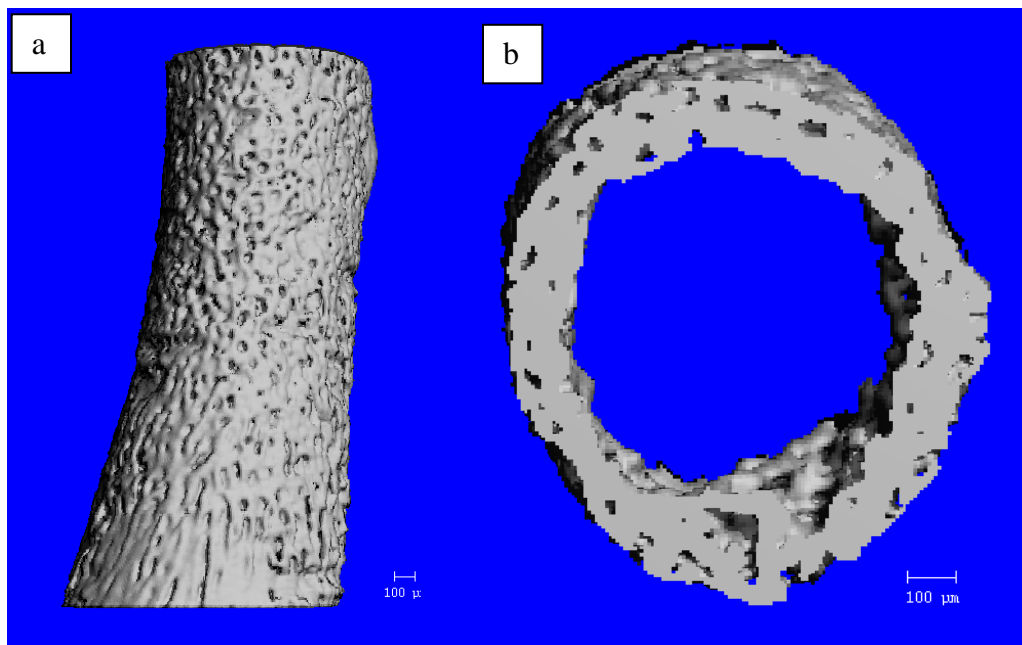
Figure 3.3.4b µCT image of femur shaft (a) and cross section of the middle 50 slices (b).

3.3.5 Structural Properties

After one week in culture, the bones underwent mechanical testing. A three-point bend test to failure was conducted using a small-scale loading machine fabricated in-house [74]. Eleven pairs (distracted vs. contralateral control) were tested for GRP I, and 9 pairs were tested for GRP II. The bones were placed with the condyles facing upward on the testing device, exposing the posterior side of femur shaft to the central loading point. The bottom supports were spaced at 2.41mm. The central loading point then came down on the posterior side of the bone shaft with a velocity of 0.38 mm/s and broke the bone in the bone shaft. A 4.535 kg load cell (Honeywell Sensotec, Columbus, OH) was used to record the forces experienced by the bone while a 25mm displacement sensor (Measurements Group Inc., Raleigh, NC) was used to record the displacement. Data was collected at a rate of 10Hz using StrainSmart Software (Vishay, Malvern, PA).

Figure 3.3.5a: 3-point bend test to failure to assess structural properties [7]

Figure 3.3.5b: Image of femur post 3-point bend test to failure showing the fracture through the bone shaft

Upon completion of the mechanical testing, load versus displacement curves were created using Microsoft Excel. The graphs were then analyzed to determine structural properties. Failure load (N) was defined as the highest point (largest load) on the curve and the displacement (mm) at this point was defined as the failure displacement. The slope of the linear portion of the graph was the stiffness (N/mm). Failure loads were converted to moments, and a moment versus displacement curve was created. Failure moments (N*mm) were then recorded and calculated by using the formula [75]

$$M = FL/4$$

Where M= bending moment

F= applied force

L= distance between two end supports

This equation is specific to the bending moment for objects undergoing 3-point bend testing. The area under the moment curve was then found using the trapezoid rule. The

area under the moment curve represents how much energy was needed to break the bone shaft.
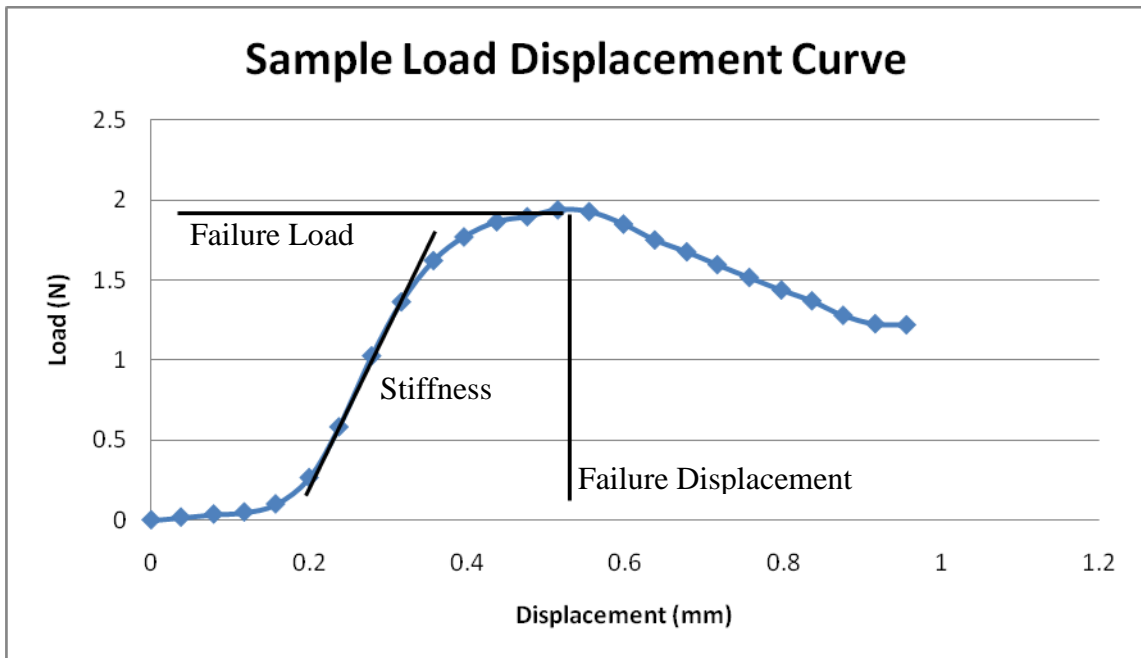
Figure 3.3.5c: Sample load displacement curve. Failure load, failure displacement, and stiffness are labeled for understanding.

3.4 Age-Matched Bones

It is recognized that the organ culture model does not perfectly mimic the living environment, and so to see how well the organ culture compared to the native environment, twelve day old Wistar rats were tested. These femurs underwent the same femur extraction as the bones from GRPs I and II except that they occurred twelve days after birth. After extraction, the bones underwent several of the tests that had been completed on the bones from GRPs I and II and all bones were imaged using the Nikon Coolpix 5400 digital camera with a Nikon SMZ645 dissecting microscope to obtain their dimensions. All bones were massed to obtain the wet mass before 11 of the bones

underwent 3-point bend testing until failure so that the structural properties could be found. With these bones, the spacing between the two bottom supports was 4.83 mm as compared to the 2.41mm spacing for the bones from GRPs I and II. Eleven bones underwent the defatting process in acetone in order that dry mass, ash mass, and ash fraction could be found, while twelve of the bones were used for µCT and areal property analysis. All of these age-matched bones were tested on the twelfth day after birth where as all of the bones from GRPs I and II were tested thirteen days after birth. Even though these are not the exact same time point, we feel these time periods are close enough that comparisons can be made between them since the exact birth of the neonates is variable.

Figure 3.4a : Comparison between organ culture bone after 1 week (L) and twelve day old bone (R).
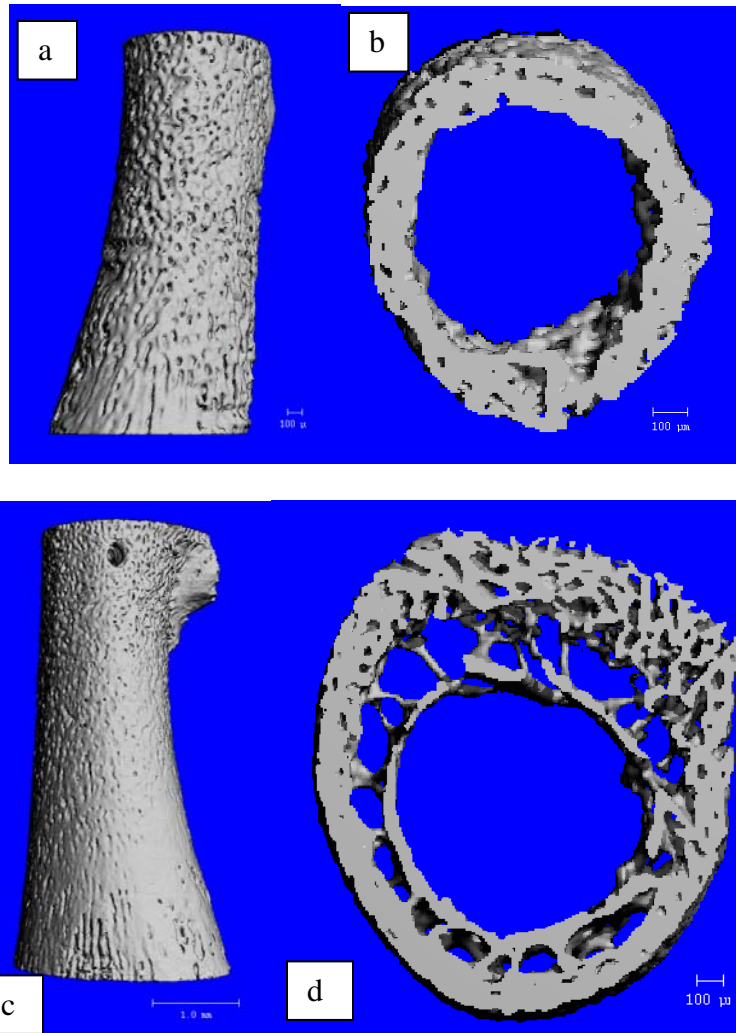
Figure 3.4b : Comparison between µCT images of organ culture bone after 1 week (a,b) and twelve day old bone (c,d).

3.5 Statistical Analysis

Statistical analysis for this experiment was completed using GraphPad Prism 5 Software (GraphPad Software, La Jolla, CA). For comparisons between distracted bones and their paired contralateral controls, a paired t-test with α=.05 was used. For comparisons between the age-matched bones and un-paired samples, an unpaired t-test with α=.05 was used. Unpaired t-tests were also run for the osteocyte viability study

since the cell counts were collectively grouped. Standard deviations were calculated for

all means and are represented by error bars on bar charts and are included in tables.

4 Results

4.1 LDH

Osteocyte viability was analyzed by comparing the changes of the treated (distracted) bones to their contralateral controls. Six longitudinal slices from three bones (18 total slices) were analyzed for the control and treated bones for both GRP I and II. GRP I displayed a 6.21% increase in LDH+ osteocytes and a 21.39% decrease in LDH- osteocytes, both of which were significantly different (p<.05). GRP II displayed a 13.02% increase in LDH+ osteocytes and a 22.04% decrease in LDH- osteocytes, both of which were significantly different (p<.01). GRP II also displayed a significant change (p<.05) for the percentage of empty lacuna between control and distracted bones with a 21.85% decrease in the number of empty lacunae in the distracted bones. The statistical bar charts (mean ± SEM) showing osteocyte viability can be seen in the following figures.
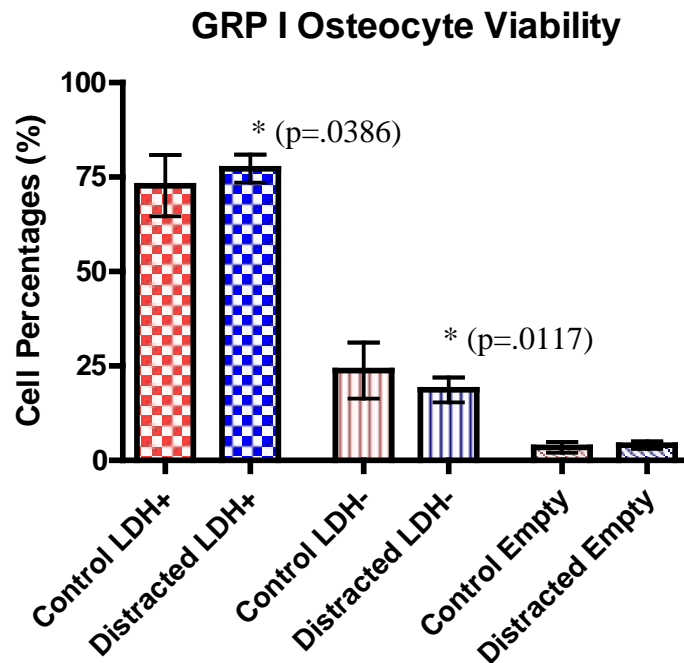
Figure 4.1a: Bar chart of osteocyte viability (mean ± SD) for GRP I.

GRPII Osteocyte Viability
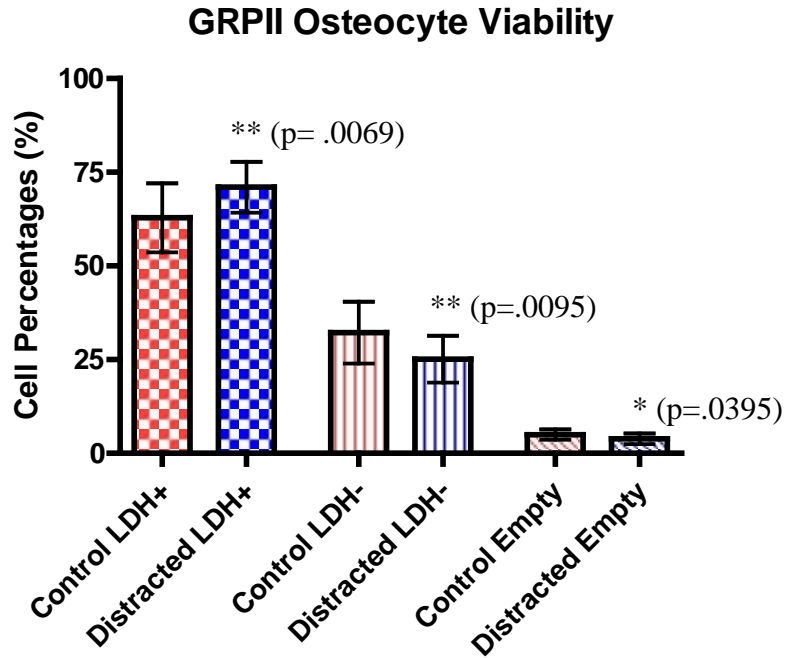
Figure 4.1b: Bar chart of osteocyte viability (mean ± SD) for GRP II.

4.2 Dimensions

Dimensions were analyzed by comparing the changes of the treated (distracted) bones to their contralateral controls and although there were no significant differences for any of the dimensional results, there were trends that were seen in both groups for all three lengths. Shaft diameter decreased 3.41% for GRP I and 3.51% for GRP II. Shaft length increased 1.41% for GRP I and 2.09% for GRP II. Total length decreased 0.32% for GRP I and 0.26% for GRP II. The dimensional data can be seen below in Table 4.2a.

Table 4.2a Dimensional Results (mean ± SD)

Group	n pairs	Shaft Diameter (mm)		Shaft Length (mm)		Total Length (mm)	
		Control	Treated	Control	Treated	Control	Treated
I	23	1.126 ± .1589	1.088 ± .1176	4.440 ± .3501	4.502 ± .3918	10.245 ± .6023	10.211 ± .6632
II	31	1.099 ± .1407	1.060 ± .1322	4.732 ± .3758	4.831 ± .3969	10.315 ± .5783	10.288 ± .7452

To show that there was growth in the control bones over the one week period, the dimensions taken from Day 1 from previously tested five day old Wistar rats (n=16) were compared to the one week controls. Unpaired t-tests were used to determine significant differences which were seen in the changes of shaft length (p<.001) and total length (p< .01). The dimensional data for changes over one week in culture can be seen below in Table 4.2b showing increases in shaft diameter, shaft length, and total length.

Table 4.2b Percent Growth in Culture

	Shaft Diameter (mm)		Shaft Length (mm)		Total Length (mm)	
	Day 1	1 WK C	Day 1	1 WK C	Day 1	1 WK C
	1.031	1.111	4.085	4.607	9.675	10.285
% Growth	7.74%		12.77%		6.31%	
p value	NS		< .0001		.0013	

4.3 Massing

Mass properties were analyzed by comparing the changes of the treated (distracted) bones to their contralateral controls. The differences between the control and treated bones for both GRP I and GRP II followed the same trends. Wet mass decreased 6.40% for GRP I and 8.88% for GRP II. Dry mass decreased 2.25% for GRP I and 0.62% for GRP II. Ash mass increased 1.60% for GRP I and 4.63% for GRP II. Ash fraction increased 2.88% for GRP I and 5.23% for GRP II. Wet, dry, and ash mass results can be seen in Table 4.3a. Ash fraction results can be seen in Table 4.3b.

Table 4.3a: Massing Results (mean ± SD)

Group	Pairs	Wet Mass (g) Control	Treated	Pairs	Dry Mass (g) Control	Treated	Pairs	Ash Mass (g) Control	Treated
I	23	0.0570 ± .0082	0.0534 ±.0102	9	0.0079 ± .0015	0.0077 ± .0012	9	0.0021 ± .0004	0.0021 ± .0004
II	31	0.0564 ± .0071	0.0514 ± .0088	9	0.0089 ± .0004	0.0089 ± .0003	9	0.0024 ± .0001	0.0025 ± .0001

Table 4.3b: Ash Fraction (mean ± SD)

Group	Pairs	Ash Fraction (%) Control	Treated
I	9	26.53 ± 2.129	27.29 ± 2.353
II	9	26.84 ± 1.613	28.24 ± 1.184

To show that there were changes in mass of the control bones over the one week

period, the masses taken from Day 1 from previously tested five day old Wistar rats

(n=20) were compared to the one week controls. Unpaired t-tests were used to determine

significant differences which were seen in the changes of wet mass (p<.05), dry mass

(p<.01), and ash mass (p< .01). The mass data for changes over one week in culture can

be seen below in Table 4.3c.

Table 4.3c Mass Changes in Culture

	Wet Mass (g)	Dry Mass (g)	Ash Mass (g)	% Ash Fraction
Day 1	0.0512	0.0070	0.0018	26.09
1 Wk C	0.0567	0.0084	0.0022	27.39
% Changes	10.75%	20.24%	22.98%	4.95%
P values	.0154	.0051	.0046	NS

4.4 Areal Properties and microCT results

Areal properties were analyzed by comparing the changes of the treated

(distracted) bones to their contralateral controls from µCT analysis (6 pairs for GRP I and

5 pairs for GRP II). The analysis includes results over the entire femoral shaft as well as

the middle 50 slices of the shaft. Consistent trends were seen for both sets of analyses.

Bone and total area increased for both GRPs I and II. The medullary area increased for

GRP I but decreased for GRP II. The ratio of bone area to total area decreased for GRP I

but increased for GRP II. Both analyses displayed significant differences in medullary

area for GRP I recording a p value less than .01 when analyzed of the entire shaft and a p

value less than .05 when analyzed over the middle 50 slices. The bone area for GRP II

also displayed significance when analyzed over the entire bone shaft ($p<.05$).

Table 4.4a µCT Areal Percent Changes

	Bone Area		Total Area		Medullary Area		BA/TA	
	GRP I	GRP II	GRP I	GRP II	GRP I	GRP II	GRP I	GRP II
Mid 50 % Change	5.69%	9.98%	11.28%	5.26%	34.10% (p=.0196)	-18.16%	-6.62%	4.81%
Shaft % Change	2.63%	13.14% (p=.0186)	8.43%	8.04%	27.76% (p=.0097)	-10.52%	-7.62%	5.07%

µCT analysis also calculated the areal and polar moments of inertias as well as

volumetric and density properties. All of the areal and polar moments displayed an

increase when comparing the treated bones to their contralateral controls. Analysis over

the entire bone shaft displayed a significant change in the bone area ($p<.05$) for GRP II.

Volumetric properties followed the same trends that were seen in the areal results. The

µCT analysis displayed a decrease in density (mg HA/ccm) for both GRPs I and II as

well as across the middle 50 slices and the entire bone shaft when comparing the treated

bones to their paired controls. The results from the middle 50 slices of the bone shaft for

GRP I showed a significant change in density (p<.05).

Table 4.4b µCT Areal Moment of Inertia Percent Changes

	Ixx		Iyy		pMOI	
	GRP I	GRP II	GRP I	GRP II	GRP I	GRP II
Mid 50% Change	14.97%	4.08%	9.50%	19.64%	12.17%	11.63%
Shaft % Change	11.38%	14.21%	6.53%	13.80% (p=.0474)	8.92%	14.00%

Table 4.4c µCT Volume Percent Changes

	Bone Volume		Total Volume		Medullary Volume		BV/TV	
	GRP I	GRP II	GRP I	GRP II	GRP I	GRP II	GRP I	GRP II
Mid 50 % Change	5.70%	9.96%	11.27%	5.26%	33.99% (p=.0195)	-18.06%	-6.62%	4.81%
Shaft % Change	3.08%	9.17%	8.31%	4.38%	25.77% (p=.0263)	-13.08%	-7.62%	5.08%

Table 4.4d µCT Density (mg HA/ccm) Changes (mean ± SD)

	Full Shaft			Shaft Middle 50		
Bone	Control	Treated	% Change	Control	Treated	% Change
GRP I	873.447 ± 66.2	818.321 ± 35.03	-6.31% (p=.0418)	857.361 ± 59.55	788.478 ± 40.98	-8.03%
GRPII	850.959 ± 58.82	810.91 ± 57.43	-4.71%	836.933 ± 61.41	788.617 ± 57.89	-5.77%

The bones that underwent µCT imaging to determine areas and moments were

also analyzed using cross sectional image analysis by simplifying the shape of the bone

into a hollow ellipse and a hollow cylinder. The following tables show the comparative

results based on which method was used to calculate the values. Two values for the polar

moment of inertia (pMOI) are given based on the radius in the x and y direction.

41

Theoretically, the x and y radius would be identical in the cylinder approximation, but since the radius measurements were not identical, two different values were calculated based on each radius.

Table 4.4e Comparing GRP I Area Moments of Inertia Based On How They Were

Calculated (mean ± SD)

	Control			Treated		
	Ellipse	Cylinder	uCT	Ellipse	Cylinder	uCT
Ixx (mm^4)	0.063 ± .0205	0.056 ± .0187	0.041 ± .0142	0.084 ± .0340	0.074 ± .0285	0.047 ± .0356
Iyy (mm^4)	0.078 ± .0258	0.087 ± .0297	0.043 ± .0154	0.112 ± .0548	0.129 ± .0717	0.047 ± .0264
pMOI (mm^4)	0.141 ± .0460	.112 (x) .174 (y)	0.083 ± .0284	0.196 ± .0873	.148 (x) .258 (y)	0.094 ± .0619

Table 4.4f Comparing GRP I Areas Based On How They Were

Calculated (mean ± SD)

	Control		Treated	
	Ellipse	uCT	Ellipse	uCT
Total Area (mm^2)	1.004 ± .1605	0.459 ± .0907	1.215 ± .3027	0.510 ± .1867
Bone Area (mm^2)	0.621 ± .1129	0.368 ± .0780	0.673 ± .1357	0.389 ± .1753
Medullary Area (mm^2)	0.383 ± .0797	0.090 ± .0345	0.542 ± .2238	0.121 ± .0372
BA/TA	0.619 ± .0522	0.804 ± .0625	0.567 ± .0980	0.751 ± .0657

Table 4.4g Comparing GRP II Area Moments of Inertia Based On How They Were

Calculated (mean ± SD)

	Control			Treated		
	Ellipse	Cylinder	uCT	Ellipse	Cylinder	uCT
Ixx (mm^4)	0.095 ± .0212	0.082 ± .0144	0.054 ± .0125	0.106 ± .0447	0.090 ± .0382	0.056 ± .0127
Iyy (mm^4)	0.133 ± .0582	0.160 ± .0904	0.051 ± .0124	0.150 ± .0744	0.179 ± .1010	0.061 ± .0045
pMOI (mm^4)	0.229 ± .0778	.164 (x) .320 (y)	0.105 ± .0220	0.256 ± .1166	.180 (x) .358 (y)	0.117 ± .0154

Table 4.4h Comparing GRP II Areas Based On How They Were

Calculated (mean ± SD)

	Control		Treated	
	Ellipse	uCT	Ellipse	uCT
Total Area (mm^2)	1.377 ± .2558	0.470 ± .0431	1.389 ± .3445	0.495 ± .0409
Bone Area (mm^2)	0.674 ± .0622	0.391 ± .0420	0.765 ± .1362	0.430 ± .0177
Medullary Area (mm^2)	0.703 ± .2350	0.079 ± .0270	0.624 ± .2828	0.065 ± .0256
BA/TA	0.500 ± .0806	0.833 ± .0628	0.568 ± .1093	0.873 ± .0468

Prior to obtaining the μCT equipment, several pairs of bones had already been cut

and analyzed to obtain their areas and moments of inertia. Those results were combined

with the image analysis results obtained after scanning in the μCT to produce the

following tables with 9 pairs of femurs used for both GRP I and II. By approximating the

bone shaft cross section as an ellipse, GRP I had significant differences in Ix ($p<.05$), Iy

($p<.05$), pMOI ($p<.05$), total area ($p<.05$), and bone area ($p<.05$). By approximating the

bone shaft cross section as a cylinder, GRP I had significant differences in Ix ($p<.05$) and

Iy (p<.05). No significant differences were seen between control and treated bones in

GRP II regardless of the approximation used.

Table 4.4i GRP I Areas and Moments Based On Elliptical

Approximation (mean ± SD)

ELLIPSE ESTIMATED				
GRP I (n=9)	Control	Treated	% Change	P Value
Total Area (mm^2)	1.070 ± .1831	1.297 ± .2703	21.19%	.0287
Bone Area (mm^2)	0.626 ± .0991	0.718 ± .1392	14.58%	.0489
Medullary Area (mm^2)	0.444 ± .1329	0.579 ± .1948	30.52%	NS
BA/TA	0.590 ± .0705	0.563 ± .0874	-4.73%	NS
Ixx (mm^4)	0.069 ± .0194	0.096 ± .0334	40.69%	.0180
Iyy (mm^4)	0.086 ± .0304	0.125 ± .0482	45.68%	.0257
pMOI (mm^4)	0.154 ± .0486	0.221 ± .0803	43.46%	.0191

.

Table 4.4j GRP I Moments Based On Cylindrical Approximation (mean ± SD)

CYLINDER ESTIMATED				
GRP I (n=9)	Control	Treated	% Change	P Value
Ixx (mm^4)	0.062 ± .0173	0.085 ± .0296	38.20%	.018
Iyy (mm^4)	0.096 ± .0392	0.143 ± .0609	48.23%	.0257

Table 4.4k GRP II Areas and Moments Based On Elliptical

Approximation (mean ± SD)

ELLIPSE ESTIMATED				
GRP II (n=9)	Control	Treated	% Change	P Value
Total Area (mm^2)	1.328 ± .2336	1.413 ± .2788	6.41%	NS
Bone Area (mm^2)	0.654 ± .0761	0.714 ± .1259	9.11%	NS
Medullary Area (mm^2)	0.673 ± .1988	0.699 ± .2483	3.79%	NS
BA/TA	0.499 ± .0613	0.516 ± .1019	3.38%	NS
Ixx (mm^4)	0.0916 ± .0236	0.1046 ± .0319	14.12%	NS
Iyy (mm^4)	0.1217 ± .0453	0.1409 ± .0553	15.79%	NS
pMOI (mm^4)	0.213 ± .0654	0.246 ± .0844	15.08%	NS

Table 4.4l GRP II Moments Based On Cylindrical Approximation (mean ± SD)

CYLINDER ESTIMATED				
GRP II (n=9)	Control	Treated	% Change	P Value
Ixx (mm^4)	0.080 ± .0218	0.091 ± .0283	13.06%	NS
Iyy (mm^4)	0.142 ± .0683	0.165 ± .0769	16.26%	NS

Although the area moments of inertia represent the bone's ability to resist load in bending, when using μCT, the section moduli (I/C, where I is the areal moment and C is the maximum radial extent in the direction perpindicular to I) are used as determinants of bending strength [73]. The results were consistent between both groups as well as between the full shaft and middle 50 slices showing increases in section moduli in both the long and short axis. The section modulus for the short axis for GRP II using the middle 50 slices saw a significant difference between the control and treated bones (p< .05).

Table 4.4m μCT % Changes of Section Moduli

	Imax/Cmax		Imin/Cmin	
Bone	% Change	P Value	% Change	P Value
GRP I Full	4.66%	NS	3.49%	NS
GRP I Mid 50	7.71%	NS	7.13%	NS
GRP II Full	13.55%	NS	11.34%	NS
GRP II Mid 50	10.12%	NS	14.56%	0.0422

4.5 Mechanical Testing

Structural properties were analyzed by comparing the changes of the treated (distracted) bones to their contralateral controls from the 3-point bend testing (11 pairs for GRP I and 9 pairs for GRP II). Trends were seen between both groups for all three structural properties. Failure load increased 9.15% for GRP I and 18.85% for GRP II. Failure displacement decreased 1.45% for GRP I and 11.49% for GRP II. Stiffness increased 31.18% for GRP I and 53.12% for GRP II. All three of these trends can be seen by looking at Figure 4.5a which illustrates the fact that the treated bone has a higher failure load, a shorter failure displacement, and a higher stiffness than the control bone.
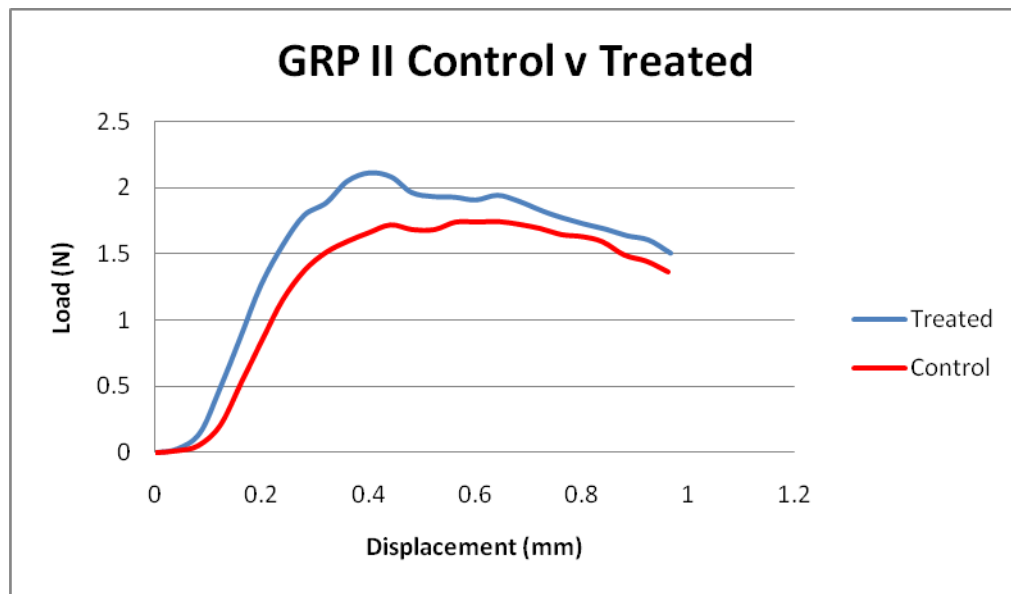
Figure 4.5a: Load displacement curve for both a control and treated bone from GRP II.

Differences in failure load between the control (C) and treated (T) populations in GRP II were significantly different (p<.01). Differences in stiffness between the control and treated populations in GRP II were significantly different (p<.001). For the analysis of structural properties, 11 pairs were tested for GRP I and 9 pairs were tested for GRP II.
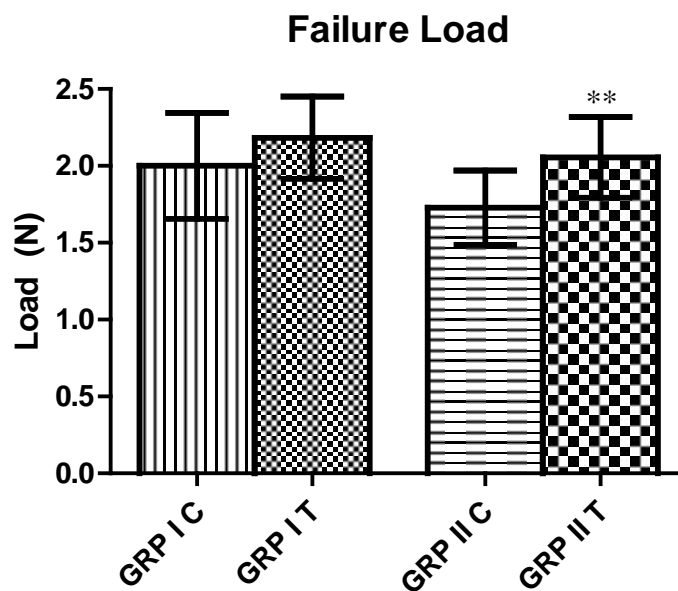
Figure 4.5b: Bar chart of failure load (mean ± SD) for GRP I and II. GRP II differences were significant (p= .0144)

Failure Displacement
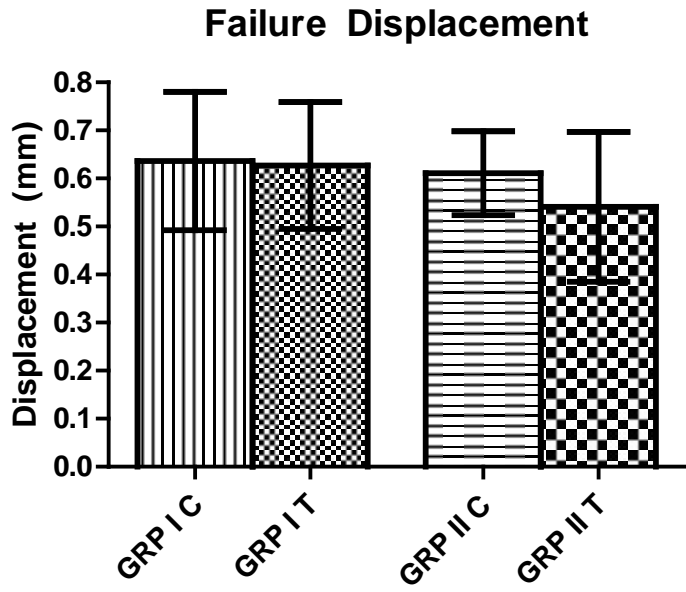
Figure 4.5c: Bar chart of failure displacement (mean ± SD) for GRP I and II.
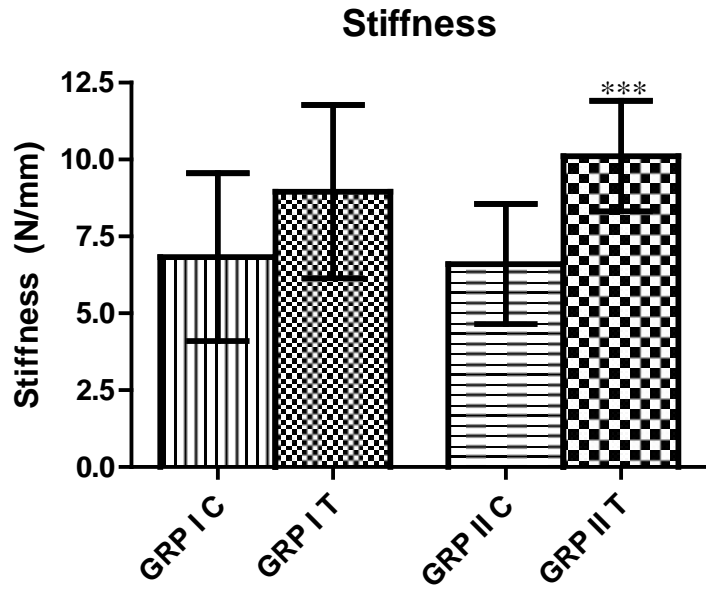
Stiffness

Figure 4.5d: Bar chart of stiffness (mean ± SD) for GRP I and II. GRP II

differences were significant (p= .0009)

Area under Moment Curves
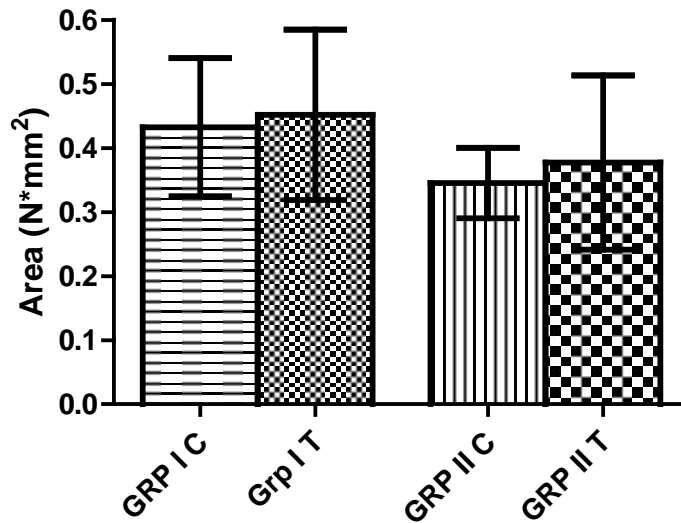
Figure 4.5e: Bar charts of area under the moment curves (mean ± SD) for GRP I and II.

Failure moment data is not presented in this section because the distances between the supports for 3-point bend testing did not change for any of the bones in GRPs I or II, as such, the data for failure moments is just a scaled representation of the data for failure load. Failure moments will be presented when comparing the bones of GRP I and II to the age-matched bones so normalized comparisons can be made between these groups.

4.6 Age Matched Data

The results taken from control bones, GRP I treated bones, and GRP II treated bones were compared against bones that were analyzed after twelve days of birth. The results are shown below in Table 4.6. As expected, every characteristic that was analyzed supported the fact that the organ culture was inferior to the age-matched bone.

Table 4.6: Percent Changes Between the Controls, GRP I Treated, and GRP II

Treated Compared to Twelve Day Old Bones.

	Control % Change	Grp I T % Change	Grp II T % Change
Moment (N*mm)	-85.61	-83.27	-84.26
Fail Displacement (mm)	-43.50	-43.32	-51.10
Moment Stiffness ((N/mm)/mm)	-78.13	-69.92	-67.20
Area Under Moment Curve (N*mm^2)	-92.46	-91.34	-92.77
Shaft Diameter (mm)	-36.59	-37.89	-39.45
Shaft Length (mm)	-25.74	-27.43	-22.14
Total Length (mm)	-24.63	-25.17	-24.61
Wet Mass (g)	-53.92	-56.61	-58.19
Dry Mass (g)	-71.23	-73.64	-69.62
Ash Mass (g)	-76.03	-77.34	-73.18
% Ash Fraction (%)	-16.55	-14.65	-11.67

Figure 4.6: Moment comparison between twelve day old bones and Grp II treated

bones.

5 Discussion

5.1 LDH

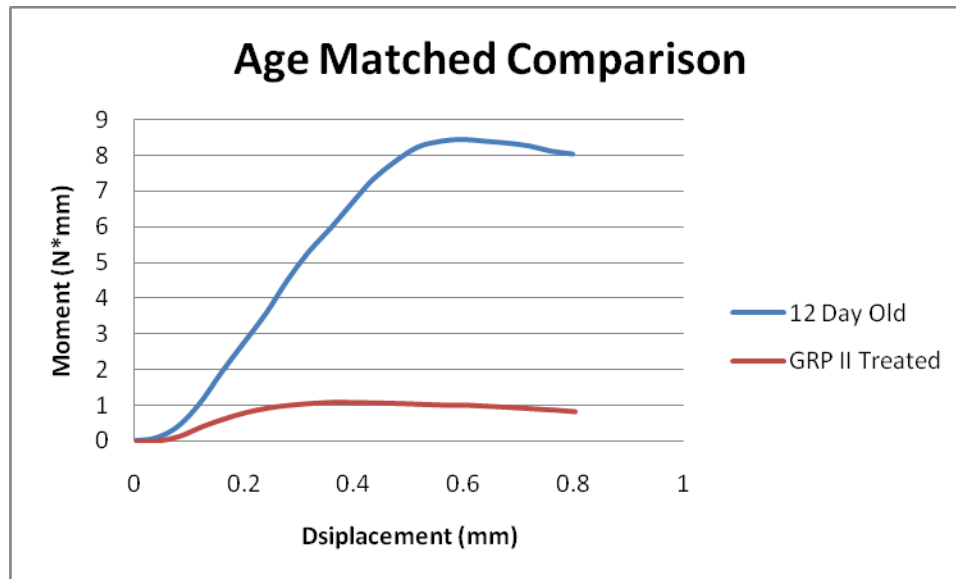Through experimentation of this model, it was shown that linear distraction on a bone in an organ culture model significantly increased the viability of the osteocytes housed within the bone matrix. This is important to note because it implies that the bone is responding on a cellular level to the application of linear distraction in the organ culture model. It is also important to note the differences between GRPs I and II. GRP II had a higher percentage of metabolizing osteocytes than GRP I. This suggests that an increase in the amount of days the bones were distracted translated directly into increased osteocyte viability.

5.2 Dimensions

In this study, there were no significant differences between changes of control versus distracted bones for either GRP I or GRP II. It must be noted that significant changes were not expected for this particular study because this study compared bones at the same time point, one week in culture. Although there were no significant differences, expected trends did occur, specifically, the shaft length increased as a result of the distraction. Additionally, the shaft diameter decreased which would not be unexpected with an increase in shaft length. This is the same pattern that would be seen on a cylindrical hollow rod, similar to the shape of a femur shaft, and although the results were not significant, the trend of lengthening in the shaft supports the successful modeling of distraction osteogenesis. Although not paired, the comparisons between day 1 bones and the one week culture controls are in agreement with the growth in culture demonstrated by Saunders' 2-day old neonatal model [7]. One unexpected result was the

51

decrease in total length between the treated and control bones. Considering there was an increase in the length of the bone shaft, one would expect there to also be an increase in the total length of the bone. Since the changes between both GRP I and GRP II were small (.32% and .26% respectively), it is possible that the differences were due to the increased handling of the distracted bones, but it seems more likely that the differences were due to small natural discrepancies in limb length.

5.3 Massing

Significant differences in bone masses were not expected because control and distracted bones were compared at the same time point. Again, trends were seen for both GRP I and GRP II in the form of decreased wet mass and dry mass. One possible explanation for the decrease in wet mass and dry mass between the control and treated bones is the fact that the treated bones had to be suture wrapped and distracted. This increase in handling led to the researcher removing strands of tissue that may have still been attached to the bone after blunt dissection. Due to the lesser extent of handling of the control group, higher masses were recorded. This handling did not factor into the ash mass since all of the tissue was incinerated in the ashing process. Ash mass and percent ash fraction increased for both groups. Although not significant, this experiment displayed that linear distraction on the bone in an organ culture model increased the mineral content of the bone. This increase in mineral content is most likely seen by an increase in calcium which correlates to the results seen for the mechanical properties. Although not paired, mass comparisons between day 1 bones and the one week culture controls are in agreement with the growth in culture demonstrated by Saunders' 2-day old neonatal model [7].

52

5.4 Areal Properties

Based on the microCT results, the treated bones resisted bending and torsion better than their paired controls. The results also displayed an increase in both bone and medullary area. Not only is it the increase in area that matters, but where along the cross section the new bone is being laid down correlates to the increases in the moments. If more bone is being laid down along the x-axis, the bending moment along the x-axis will be higher. By looking at the section moduli as well as the area moments, the bone's ability to withstand bending in both the long and short axis of the bone increased. This also corresponds to the increased failure load in bending seen with the 3-point bend test.

By using an ellipse based approximation, significant differences were seen in multiple areal characteristics, but these results were overshadowed by the fact that the µCT did not show the same significance. The µCT uses a more accurate approach to solving for areas and moments whereas the ellipse and cylinder based approximations are much simpler. The µCT results showed the same trends, but they were more accurate compared to the approximations meaning that the significance seen in the approximations were due to overestimations. Taking this into the consideration, further use of this system should only include results obtained using the µCT.

5.5 Mechanical Testing

By performing mechanical testing (3-point bending), structural properties of the bone were determined. Throughout both groups, the distracted bones displayed an increase in failure load, a decrease in failure displacement, and an increase in stiffness. This increase in failure load suggests that the bone will be able to withstand higher loads, while this decrease in failure displacement suggests that while being loaded in bending,

53

the bone will not displace as much. Putting together the increase in resistance to load and the decrease in deformation suggests that the bones are getting stronger as well as stiffer. This study verified this increase in stiffness. The increase in area under the moment versus displacement graphs showed that more energy was required to break the bones.

One reason why the treated bones were able to withstand more load is due to the fact that the treated bones had an increase in mineral content. It is the minerals (along with collagen) that give bone a combination of flexibility and strength with more mineral content equating to more strength [30]. The increased resistance to bending was also supported by the μCT data showing that the increased bone area resulted in more strength.

5.6 Age-Matched Bones

The control and treated bones from this study were compared to bones of the same age that were left in vivo. This comparison was meant to indicate the effectiveness of the organ culture. By physical appearance alone, it was obvious that the age-matched bones were much longer, thicker, and heavier than either the control or treated organ culture bones. Although these results were expected, it was hoped that the treated and control bones would better correlate to the age-matched bones.

One reason why the age-matched bones were so much stronger and could resist more load may be due to the fact that the bones receive more calcium while still in the body than they do through the organ culture system. Although the organ culture model is a biomimetic environment, our system has no supply of blood or calcium. In vivo, the blood supply provides a means for the bone to receive nutrients and minerals such as calcium which help it grow and resist load [30]. This extra week of growth within the

body enables the bone to be more calcified as was seen in the increase in mineral content over the organ cultured bones.

5.7 Concerns

This study tried to mimic the distraction osteogenesis process, but there are some areas of concern. One such area of concern is that the suture was removed from the femurs after the two hour distraction period occurred. In a real clinical setting, the hardware is left attached to the patient until the entire distraction process is completed. Therefore, by removing the suture, it leaves the possibility that the next tension loading will not occur in the same exact direction or location on the bone. As noted in 2.3.1, it is known that changes in loading direction can change both stiffness and strength [53]. Since our model was linear, it probably did not have much of an effect on the loading direction. Secondly, since the clinical hardware is not removed, it does not allow the possibility of the bone growth to retract. In fact, it has been shown that very little change in the baseline force occurs while using quasi-continuous distraction meaning the bone is feeling a consistent force over the course of the day [76]. In clinical settings, the distraction is held in place by the hardware whereas our system completely removes any forces still acting on the bone.

By using an organ culture to model distraction osteogenesis, we were able to eliminate any systemic effects. One problem with this method is the possibility of systemic effects that could be beneficial to the distraction process. One example would be weight bearing for patients who undergo distraction osteogenesis on their legs. It has been shown that bone formation and mineralized tissue were better in groups that underwent weight bearing as compared to those that did not [45]. Since this study was a

proof concept, not including the possible benefits of systemic effects was intended. This is something that could be looked at in the future, but weight bearing patients are just one subset of patients when dealing with distraction osteogenesis. Removing the systemic effects gives us a better understanding of what is actually occurring through the distraction process.

One characterization of distraction osteogenesis is the profuse increase in vascularization in which endothelial progenitor cells contribute to the bone regeneration [77]. The actual effect of this increase is unknown; however, it is certain that the neovascularization process is essential for successful bone formation during distraction osteogenesis [77]. In this organ culture model, a vascular system is not present. Cultured medium is present, but it cannot replicate a vascular system. It does not deliver minerals and nutrients normally seen in the body, and the lack of a vascular system is one reason why the viability of the bones drops in culture.

One concern that has been raised is the amount of pairs that were tested for each method of analysis. Funding limitations limited the number of animals that could be tested. Since this experiment was a proof of concept, the animals were split among the different testing methods. A retroactive power analysis was conducted to see if significance would occur with more samples. The power analysis (α=5%, β=50%) showed that increasing the sample size to 20 pairs should increase significance in many of the μCT properties including the area and polar moments of inertia for GRP II. Since the μCT analysis provided the most information, it would be beneficial to conduct a distraction experiment based solely on obtaining μCT results.

5.8 Future Work

The outcomes from this study leave more questions to be answered in future work. One area of improvement would be to make the loading regimes more clinically relevant. This system was designed as a proof of concept to elicit a response by choosing two extremes as the loading regimes. In this study, distraction occurred over a two hour period once a day, while in the clinic it is common to see several distractions per day. One thing to take into consideration is that by handling the bones more often, the possibility for contamination increases. By making the distraction more clinically relevant while still avoiding contamination, the results will better predict what is happening during distraction osteogenesis in the clinical setting as well as providing the potential for procedural optimization.

The biggest change that should be made in the future and one that was initially overlooked is with the loading device itself, as the current system does not allow for data acquisition or programming during distraction. A better system should have been developed in order to allow for recording of loads and distraction rate while the distraction was occurring. The current system relies on the researcher to physically turn a screw to distract the bones, which leaves the possibility of having variables that may affect the distraction process. The biggest problem from this is that the distraction rate may not be the same for every distraction. By having a system that allows for data capture and programming, the distraction rate can be set and the machine will ensure constant rates throughout all distractions. It will also display more accurately the stress relaxation in the system. The testing machine used for the 3-point bend tests [74] has the capabilities needed to perform this distraction if it could be housed in a sterile environment. Due to the fragile nature of the bones, it is believed that any hardware that

would come in contact with the bones would destroy them. Continuing with the suture wrapping technique would be best, however a second set of sutures should be tied and pulled on the posterior side of the femurs to limit the bending effect. This will allow for the bone shaft to experience a more linear tensile force. Because the bones are returned to the organ culture after distraction, the use of a strain gage to measure the strain on the shaft during each distraction is not possible. This study found what distraction distance should produce a 2% strain on the shaft based on previously tested dimensions. If the researcher wants to know the level of strain for each bone being distracted, a microscope and camera (Nikon Coolpix 5400 digital camera and Nikon SMZ645 Dissecting microscope, Nikon Instruments Inc., Melville, NY) could be set up inside the sterile hood to take images before and after straining. Based on the changes in shaft length obtained from image analysis (Image J Software, NIH), a strain could be calculated.

Because of the higher potential for contamination and the need for age matched pairs, this study did not look at the overall growth of the bone over the one week culture period. Rather, this study compared the final lengths of control and treated bones. Although previous data was compared to the current data to display changes in length over time, a paired study should be conducted to measure the length before and after the distraction occurs to gain a better understanding of how much growth can occur with distraction osteogenesis. This will help to determine what is happening clinically and may also lead to an optimization of distraction.

This study looked at the simplest form of distraction: a one directional, linear distraction on the femur. In the clinical setting, very rarely is distraction osteogenesis that simple, especially in cranio-maxillofacial distraction. There are usually other forces

acting on the bone, particularly muscle forces in multiple directions. There are also bones with much more complex shapes that may result in the need for multi-directional distraction. Expanding this model to include multiple forces, multiple loading directions, and different bones will also make it more clinically relevant. Since there have been clinical studies conducted on mandibles where no osteotomy or corticotomy was needed [47], the next bone to be studied in an organ culture distraction model should be the mandible. This would require the inclusion of multiple forces in multiple directions. The simplest mandible model would include two distractors that pulled the bone in the x and y directions, however, to be more accurate to the muscle forces acting on the bone, the angle of the distraction should be able to be rotated.

One potential outcome of the study is the application of using distraction at the bone-implant interface to increase osseointegration. It has been determined that mechanical loading factors at the bone-implant interface are critical for the osseointegration and clinical success of the implant [78]. However, Kokkinos' study did not look at using strain as a means of mechanical loading, but rather used four-point bending as their mechanical loading. The study found that mechanical load contributed to the regulation of osteoblast differentiation helping osseointegration. If strain was also found to increase the regulation of osteoblast differentiation, the potential for using tension for better osseointegration at the bone-implant interface would exist. Winwood, et al, [49] also saw the potential correlation between strain and osseointegration by stating that strain related bone deposition and bone induction may critically affect the chances for osseointegration.

6 Conclusions

The primary aim of this study was to develop an organ culture system to model distraction osteogenesis. The results from this study prove that distraction osteogenesis can be modeled in an organ culture system using neonatal rat femurs. The second aim of this study was to determine if the organ culture distraction osteogenesis model would induce bone growth or have other effects on the bone. Although not significant, there were changes in the length of the bone shaft. Significant differences were also seen with the increase in osteocyte viability, the bones' ability to withstand more loading in bending, the increased stiffness, and several µCT results. These results demonstrate that the bone and the bone cells respond to applications of linear distraction in our distraction osteogenesis model.

References

1. Carinci, F., F. Pezzetti, et al., *An in vitro model for dissecting distraction osteogenesis*. Journal of Craniofacial Surgery, 2005. 16(1): 71-78.
2. Ai-Aql, Z. S., A. S. Alagl, et al., *Molecular mechanisms controlling bone formation during fracture healing and distraction osteogenesis*. Journal of Dental Research, 2008. 87(2): 107-118.
3. Reina-Romo, E., M. J. Gomez-Benito, et al., *Modeling distraction osteogenesis: analysis of the distraction rate*. Biomechanics and Modeling in Mechanobiology, 2009. 8(4): 323-335.
4. Bhatt, K. A., E. I. Chang, et al., *Uniaxial mechanical strain: An in vitro correlate to distraction osteogenesis*. Journal of Surgical Research, 2007. 143(2): 329-336.
5. Askari, M., J. S. Gabbay, et al., *Favorable morphologic change of preosteoblasts in a three-dimensional matrix with in vitro microdistraction*. Plastic and Reconstructive Surgery, 2006. 117(2): 449-457.
6. Glucksmann, A., The *role of mechanical stresses in bone formation in vitro.* Journal of Anatomy, 1942. 76: 231-239.
7. Saunders, M. M., L. A. Simmerman, et al. *Biomimetic bone mechanotransduction modeling in neonatal rat femur organ cultures: structural verification of proof of concept*. Biomech Model Mechanobiol, 2010.
8. Alm, R., L. Edvinsson, et al., *Organ culture: a new model for vascular endothelium dysfunction*. BMC Cardiovascular Disorders, 2002. 2(1): 8.
9. Takezawa, T., M. Inoue, et al., *Concept for organ engineering: A reconstruction method of rat liver for in vitro culture*. Tissue Engineering, 2002. 6(6): 641-650.
10. Merrick, A. F., L. D. Shewring, et al., *Organ culture of arteries for experimental studies of vascular endothelium in situ*. Transplant Immunology, 1997. 5(1): 3-9.
11. Merrilees, M. J. and L. J. Scott, *Effects of endothelial removal and regeneration on smooth-muscle glycosaminoglycan synthesis and growth in rat carotid-artery in organ-culture*. Laboratory Investigation, 1985. 52(4): 409-419.
12. Merrilees, M. J. and L. Scott, *Organ-culture of rat carotid-artery - maintenance of morphological-characteristics and of pattern of matrix synthesis*. In Vitro-Journal of the Tissue Culture Association, 1982. 18(11): 900-910.
13. Shamsuddin, A. K. M., L. A. Barrett, et al., *Long-term organ-culture of adult-rat colon*. Pathology Research and Practice, 1978. 163(4): 362-372.
14. Stepitak.M and Dolezalo H., *Organ culture of rat skeletal muscle subjected to intermittent activity.* Experientia, 1968. 24(9): 971ff.
15. Miledi, R., O. A. Trowell, *Acetylcholine sensitivity of rat diaphragm maintained in organ culture.* Nature, 1962. 194(4832): 981ff.
16. Ishizeki, K., M. Takigawa, et al., *Meckel's cartilage chondrocytes in organ culture synthesize bone-type proteins accompanying osteocytic phenotype expression*. Anatomy and Embryology, 1996. 193(1): 61-71.
17. Wetzel, D. M. and M. M. Salpeter, *Fibrillation and accelerated achr degradation in long-term muscle organ-culture*. Muscle & Nerve, 1991. 14(10): 1003-1012.

61

18. Weiss, A., E. Livne, et al., *Growth and repair of cartilage - organ-culture system utilizing chondroprogenitor cells of condylar cartilage in newborn mice.* Journal of Bone and Mineral Research, 1988. 3(1): 93-100.
19. Voisard, R., R. Baur, et al*., A perfused renal human organ culture model: Impact of monocyte attack*. Medical Science Monitor, 2007. 13(2): CR82-CR88.
20. Swanson, N., Q. Javed, et al., *Human internal mammary artery organ culture model of coronary stenting: a novel investigation of smooth muscle cell response to drug-eluting stents*. Clinical Science, 2002. 103(4): 347-353.
21. Voisard, R., B. Reinhardt, et al., *A human arterial organ culture model for investigations of functional and molecular consequences of cytomegalovirus-infection in early atherosclerosis and restenosis*. European Heart Journal, 2000. 21: P998
22. Jones, R. T., L. A. Barrett, et al., *Method for long-term organ-culture of human and bovine pancreatic ducts*. Laboratory Investigation, 1976. 34(3): 321-321.
23. Gonzalez, K., W. J. Mergner, et al., *Studies on pathogenesis of atherosclerosis - organ-culture of rabbit aorta*. Laboratory Investigation, 1979. 40(2): 257-257.
24. Del Rizzo, D. F., M. C. Moon, et al., *A novel organ culture method to study intimal hyperplasia at the site of a coronary artery bypass anastomosis*. Annals of Thoracic Surgery, 2001. 71(4): 1273-1279.
25. Lyubimov, E. V. and A. I. Gotlieb, *Smooth muscle cell growth in monolayer and aortic organ culture is promoted by a nonheparin binding endothelial cell-derived soluble factors.* Cardiovascular Pathology, 2004. 13(3): 139-145.
26. Jubb, R. W., *Effect of hyperoxia on articular tissues in organ-culture*. Annals of the Rheumatic Diseases, 1979. 38(3): 279-286.
27. Fell, H. B. and R. W. Jubb, *Effect of synovial tissue on breakdown of articular-cartilage in organ-culture*. Arthritis and Rheumatism, 1977. 20(7): 1359-1371.
28. Matsuno, M., K. I. Hata, et al., *In vitro analysis of distraction osteogenesis*. Journal of Craniofacial Surgery, 2000. 11(4): 303-307.
29. Athanasiou, K. A., C. F. Zhu, et al., *Fundamentals of biomechanics in tissue engineering of bone*. Tissue Engineering, 2000. 6(4): 361-381.
30. Salidin, Kenneth S. Human Anatomy, Second Edition. Boston, MA: McGraw Hill, 2008.
31. Saunders, M. M. and J. S. Lee, *The influence of mechanical environment on bone healing and distraction osteogenesis*. Atlas Oral and Maxillofacial Surgery Clinics of North America, 2008. 16(2): 147-58.
32. Jacobs, C. R., *The mechanobiology of cancellous bone structural adaptation*. Journal of Rehabilitation Research and Development, 2000. 37(2): 209-216.
33. Pearson, O. M. and D. E. Lieberman., *The aging of Wolff's "law": ontogeny and responses to mechanical loading in cortical bone*. American Journal of Physical Anthropology, 2004. Suppl 39: 63-99.
34. Martin RB, Burr DB, Sharkey NA. Skeletal tissue mechanics. New York: Springer-Verlag, Inc, 1998.
35. Wolff J. The law of bone remodeling [translated from the 1892 original, Das Gesetz der Transformation der Knochen, by P. Maquet and R. Furlong]. Berlin: Springer Verlag. 1986.

36. Kozlovskaya, I.B., Kreidich, Yu. V., Oganov, V.S. & Koserenko, O.P., *Pathopysiology of motor functions in prolonged manned space flights.* Acta Astronautica, 1981. 8, 1059-1072.

37. Krahl, H., U. Michaelis, et al., *Stimulation of bone-growth through sports - a radiologic investigation of the upper extremities in professional tennis players.* American Journal of Sports Medicine, 1994. 22(6): 751-757.

38. Djasim, U. M., B. J. Mathot, et al., *Histomorphometric comparison between continuous and discontinuous distraction osteogenesis.* Journal of Cranio-Maxillofacial Surgery, 2009. 37(7): 398-404.

39. Jiang, X., S. Zou, et al., *bFGF-Modified BMMSCs enhance bone regeneration following distraction osteogenesis in rabbits.* Bone, 2010. 46 (4) 1156-1161.

40. Codivilla, A., *The Classic On the Means of Lengthening, in the Lower Limbs, the Muscles and Tissues Which are Shortened Through Deformity* (Reprinted from J Bone Joint Surg Am., vol s2, pg 353-369, 1905). Clinical Orthopaedics and Related Research, 2008. 466(12): 2903-2909.

41. Ilizarov, G. A., *The tension-stress effect on the genesis and growth of tissues: Part II. The influence of the rate and frequency of distraction.* Clinical Orthopaedics and Related Research, 1989. (239): 263-85.

42. Ilizarov, G. A., *The tension stress effect on the genesis and growth of tissues .1. the influence of stability of fixation and soft-tissue preservation.* Clinical Orthopaedics and Related Research, 1989. (238): 249-281.

43. Rowe, N. M., B. J. Mehrara, et al., *Rat mandibular distraction osteogenesis: Part I. Histologic and radiographic analysis.* Plastic and Reconstructive Surgery, 1998. 102(6): 2022-32.

44. Karaharju-Suvanto, T., J. Peltonen, et al., *Distraction osteogenesis of the mandible. An experimental study on sheep.* International Journal of Oral and Maxillofacial Surgery, 1992. 21(2): 118-21.

45. Leung, K. S., W. H. Cheung, et al., *Effect of weightbearing on bone formation during distraction osteogenesis.* Clinical Orthopaedics and Related Research, 2004. (419): 251-257.

46. Staffenberg, D. A., R. J. Wood, et al*., Midface distraction advancement in the canine without osteotomies.* Annals of Plastic Surgery, 1995. 34(5): 512-7.

47. Graewe, F. R., J. A. Morkel, et al., *Midface Distraction Without Osteotomies in an Infant With Upper Respiratory Obstruction.* Journal of Craniofacial Surgery, 2008. 19(6): 1603-1607.

48. Greene, D. A. and G. A. Naughton , *Adaptive skeletal responses to mechanical loading during adolescence.* Sports Medicine, 2006. 36(9): 723-732.

49. Winwood, K., P. Zioupos, et al., *Strain patterns during tensile, compressive, and shear fatigue of human cortical bone and implications for bone biomechanics.* Journal of Biomedical Materials Research Part A, 2006. 79A(2): 289-297.

50. Lanyon, L. E., Rubin, et al., *Osteocytes, Strain Detection, Bone Modeling and Remodeling.* Calcified Tissue International, 1993. 53: S102-S107.

51. Taylor, A. F., M. M. Saunders, et al., *Mechanically stimulated osteocytes regulate osteoblastic activity via gap junctions.* American Journal of Physiology-Cell Physiology, 2007. 292(1): C545-C552.

52. Nyman, J. S., A. Roy, et al., *Mechanical behavior of human cortical bone in cycles of advancing tensile strain for two age groups*. Journal of Biomedical Materials Research Part A, 2009. 89A(2): 521-529.

53. Voide, R., G. H. van Lenthe, et al., *Femoral stiffness and strength critically depend on loading angle: a parametric study in a mouse-inbred strain*. Biomedizinische Technik, 2008. 53(3): 122-129.

54. Van Sickels. Personal Interview. 22 Mar. 2009.

55. Mandell, D. L., R. F. Yellon, et al., *Mandibular distraction for micrognathia and severe upper airway obstruction*. Archives of Otolaryngology-Head & Neck Surgery, 2004. 130(3): 344-348.

56. Ilizarov, G. A., V. I. Lediaev, et al., *The course of compact bone reparative regeneration in distraction osteosynthesis under different conditions of bone fragment fixation (experimental study)*. Eksp Khir Anesteziol (1969) 14(6): 3-12.

57. Choi, I. H., J. S. Shim, et al., *Effect of the distraction rate on the activity of the osteoblast lineage in distraction osteogenesis of rat's tibia. Immunostaining study of the proliferating cell nuclear antigen, osteocalcin, and transglutaminase* C. Bull Hosp Jt Dis, 1997. 56(1): 34-40.

58. Farhadieh, R. D., M. P. Gianoutsos, et al., *Effect of distraction rate on biomechanical, mineralization, and histologic properties of an ovine mandible model*. Plastic Reconstructive Surgery, 2000. 105(3): 889-95.

59. King, G. J., Z. J. Liu, et al., *Effect of distraction rate and consolidation period on bone density following mandibular osteodistraction in rats*. Archives of Oral Biology, 2003. 48(4): 299-308.

60. Snyder, C. C., G. A. Levine, et al., *Mandibular lengthening by gradual distraction. Preliminary report.* Plastic Reconstructive Surgery, 1973. 51(5): 506-8.

61. Mccarthy, J. G., J. Schreiber, et al., *Lengthening the Human Mandible by Gradual Distraction.* Plastic and Reconstructive Surgery, 1992. 89(1): 1-8.

62. Singare, S., D. Li, et al*., The effect of latency on bone lengthening force and bone mineralization: an investigation using strain gauge mounted on internal distractor device*. Biomedical Engineering Online, 2006. 5: 18.

63. Garrett, I. R., *Assessing bone formation using mouse calvarial organ cultures*. Methods in Molecular Medicine, 2003. 80: 183-98.

64. Meghji, S., Hill, P.A., Harris, M., *Bone Organ Cultures*. In: Henderson B, Arnett T (eds) Methods in Bone Biology. New York: Thomson Science, 1998.

65. Sigma Aldrich. *Fetal Bovine Serum (FBS).* 2010; Available from: http://www.sigmaaldrich.com/life-science/cell-culture/cell-culturezproducts.html?TablePage=9628642

66. Mann, V., C. Huber, et al., *The influence of mechanical stimulation on osteocyte apoptosis and bone viability in human trabecular bone*. J Musculoskelet Neuronal Interact, 2006. 6(4): 408-17.

67. Wong, S. Y. P., C. R. Dunstan, et al., *The Determination of Bone Viability - a Histochemical Method for Identification of Lactate-Dehydrogenase Activity in Osteocytes in Fresh Calcified and Decalcified Sections of Human-Bone*. Pathology, 1982. 14(4): 439-442.

68. Vector. *Methyl Green Nuclear Counterstain.* 2009. Available from vectorlabs.com/data/protocols/H3402.pdf

69. Mikic, B., M. C. H. Vandermeulen, et al. *Long-bone geometry and strength in adult bmp-5 deficient mice*. Bone, 1995. 16(4): 445-454.

70. Edwards, Charles H., <u>Historical Development of the Calculus</u>. New York, NY: Springer-Verlag New York, 1979.

71. Beer, Ferdinand P., Johnston, E. Russell, Clausen, William E. <u>Vector Mechanics for Engineers, Dynamics.</u> Boston, MA: McGraw Hill, 2007.

72. Baylor College of Medicine. *Recommended sample preparation procedure for samples to be scanned by MicroCT*. Available from: www.bcm.edu/boneprogram/?PMID=8071.

73. Bagi, C. M., N. Hanson, et al., *The use of micro-CT to evaluate cortical bone geometry and strength in nude rats: Correlation with mechanical testing, pQCT and DXA*. Bone, 2006. 38(1): 136-144.

74. Saunders, M. M. and H. J. Donahue, *Development of a cost-effective loading machine for biomechanical evaluation of mouse transgenic models*. Medical Engineering & Physics, 2004. 26(7): 595-603.

75. Yuehuei H. An, Draughn, Robert A., <u>Mechanical Testing of Bone and the Bone-Implant Interface.</u> Boca Raton, FL: CRC Press, 2000.

76. Ohnishi, I., T. Kurokawa, et al., *Measurement of the tensile forces during bone lengthening*. Clin Biomech (Bristol, Avon), 2005. 20(4): 421-7.

77. Lee, D. Y., T.-J. Cho, et al. *Distraction osteogenesis induces endothelial progenitor cell mobilization without inflammatory response in man*. Bone, 2010. 46(3): 673-9.

78. Kokkinos, P. A., I. K. Zarkadis, et al., *Effects of physiological mechanical strains on the release of growth factors and the expression of differentiation marker genes in human osteoblasts growing on Ti-6Al-4V*. Journal of Biomedical Materials Research Part A, 2009. 90A(2): 387-395.

Vita

Bradley Robert Heil was born on March 9, 1986 in Columbus, Ohio. He received his Bachelor of Science degree in Biosystems and Agricultural Engineering at the University of Kentucky in Lexington, Kentucky in May of 2008 while also graduating from the Honors Program. He began his Masters program at the Center for Biomedical Engineering at the University of Kentucky in Lexington, Kentucky in August of 2008. While attending the Center for Biomedical Engineering, he presented a poster at the 2009 UK/CWRU Biomaterials Day as well as at the 2009 BMES Annual Meeting. He also served as the secretary of the UK chapter of the Biomedical Engineering Society.